
Center in Busan APEC Cimate Center in Busan APEC Cimate Center in Busan APEC Cimate Center in Busan APEC Cimate Center in Busan APEC Cimate Center in Busan APEC Cimate Center in Busan APEC Cimate Center in Busan APEC Cimate Center in Busan
야경투시도
The relationship between the Indian Ocean Dipole-El Niño
주경투시도

Datasets

- Monthly GISST (1871-1998)
- NCEP/NCAR circulation reanalysis (1958-1998).

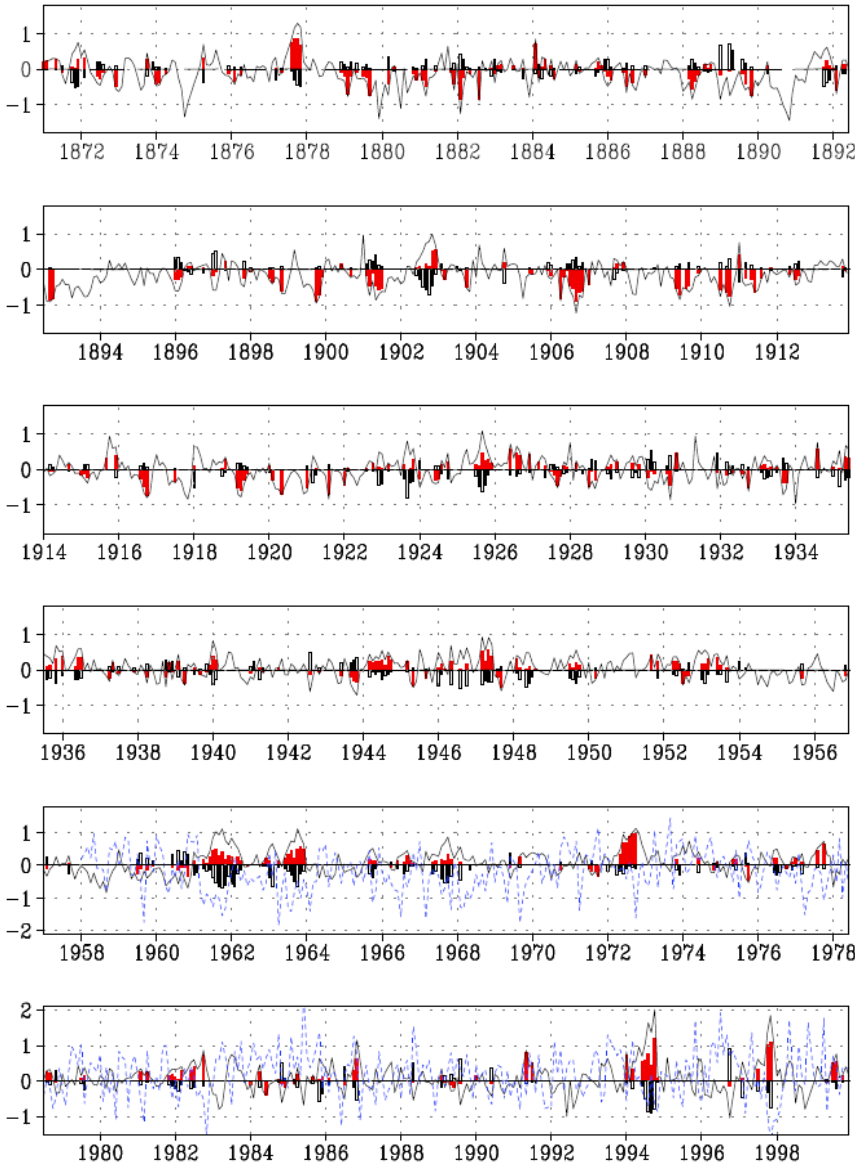

Fig. 1: The time-series of SSTA (in unit of oC) averaged over Box A (50oE-70oE, 10oS- 10oN; filled bars) and over Box B (90oE- 110oE, 10oS-equator; clear bars) during the dipole months. The sign of the SSTA over box A and that over Box B are opposite during these months. The black solid line is the Indian Ocean Dipole Mode Index,. The normalized equatorial zonal wind index (to be multiplied by 1.5; in m·s-1) defined by Saji et al.(1999), from 1958-1998, is shown as the dashed line.

Table 1. Dipole month statistics (I_{NINO3} is the NINO3 index and I_{IODM} is the IOD index. The term "single month" designates lone dipole months that do not have another preceding or succeeding dipole month).

	Total number of the months during when the I_{IODM} is significant	Total number of the months when both the I_{IODM} and I_{NINO3} are significant	Months when only I_{IODM} is significant	Single months	Single months that co-occur with ENSO
April–November	169	46	123	38	11
September–November	71	25	46	13	4
April–August	98	21	77	25	7

What the monthly stratification of the indices says

- Of the 1536 months during our study period, the IOD type of SSTA can be seen in the Indian Ocean during 498 months (see Fig. 1).

- Table 1:During April–November months of the study period, 27% of the dipole months are associated with simultaneous ENSO months. During the months of April–August, only about 21% of the dipole months are associated with ENSO months. During September–November, the dipole months co-occurring with an ENSO month amount to 35% of the total dipole months. We note that the co-occurrence refers to the simultaneous occurrence of the positive IOD phenomenon with an El Niño, or that of a negative IOD phenomenon with a La Niña. Actually, there are some years when this relationship is not valid. It is interesting to note that there are some years when a warm ENSO event (El Niño) is associated with a positive IOD event (as in 1997), while there are some years when the El Niño events co-occur with a negative IOD event (e.g. 1909, 1992). Similarly, some cold ENSO events (La Niña), such as in 1967, are accompanied by positive IOD events.

- Table 1 shows that the number of the designated dipole months is more during April–August, the developing season of the IOD (Saji et al., 1999), than those during the SON, the mature phase of the IOD events (Saji et al., 1999). Also, ENSO events generally tend to be stronger during SON, as compared to the period between April–August. These factors also indicate that not all IOD events may have been triggered by the ENSO. The fact that the number of the dipole months is more during April–August is understandable, as some of them do not develop into fully mature IOD events.

IOD circulation is independent of tropical Pacific circulation

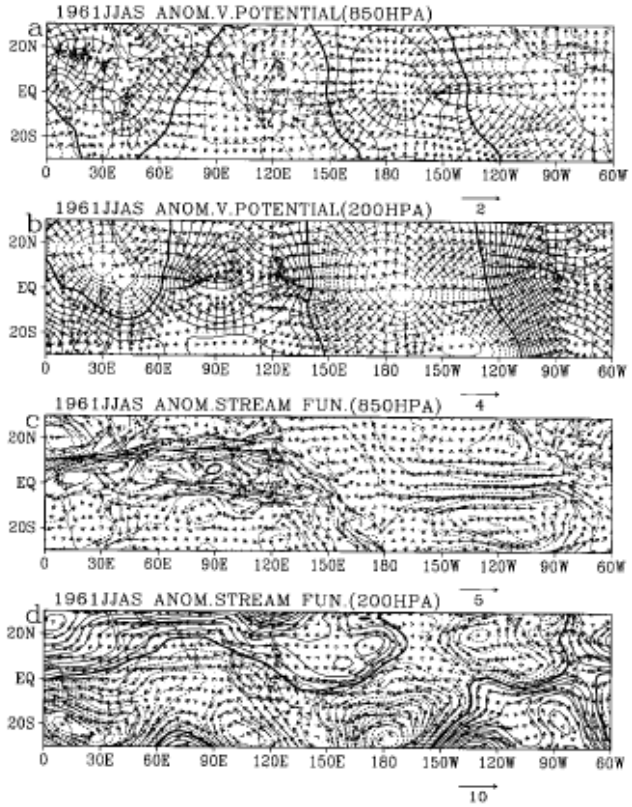

Fig. 2. The anomalous atmospheric field in 1961 during summer months (JJAS) (a) Velocity potential at 850 hPa, in $m^2 \cdot s^{-1}$ (b) Velocity potential at 200 hPa, in $m^2 \cdot s^{-1}$ (c) Streamfunction at 850 hPa, in $m^2 \cdot s^{-1}$ (d) Streamfunction at 200 hPa, in $m^2 \cdot s^{-1}$. The nondivergent wind vectors are in $m \cdot s^{-1}$.

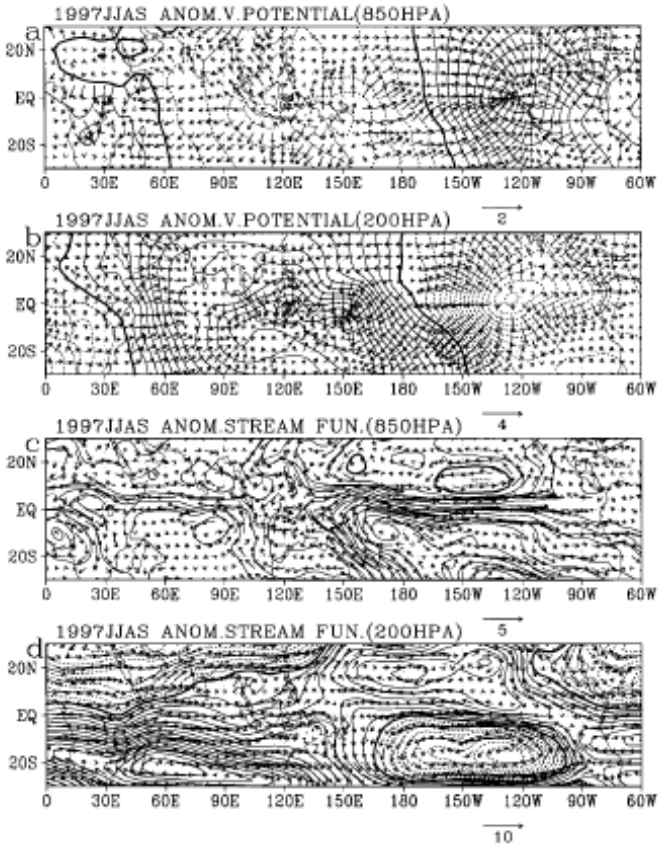

Fig. 3. Same as Fig. 2, but during 1997.

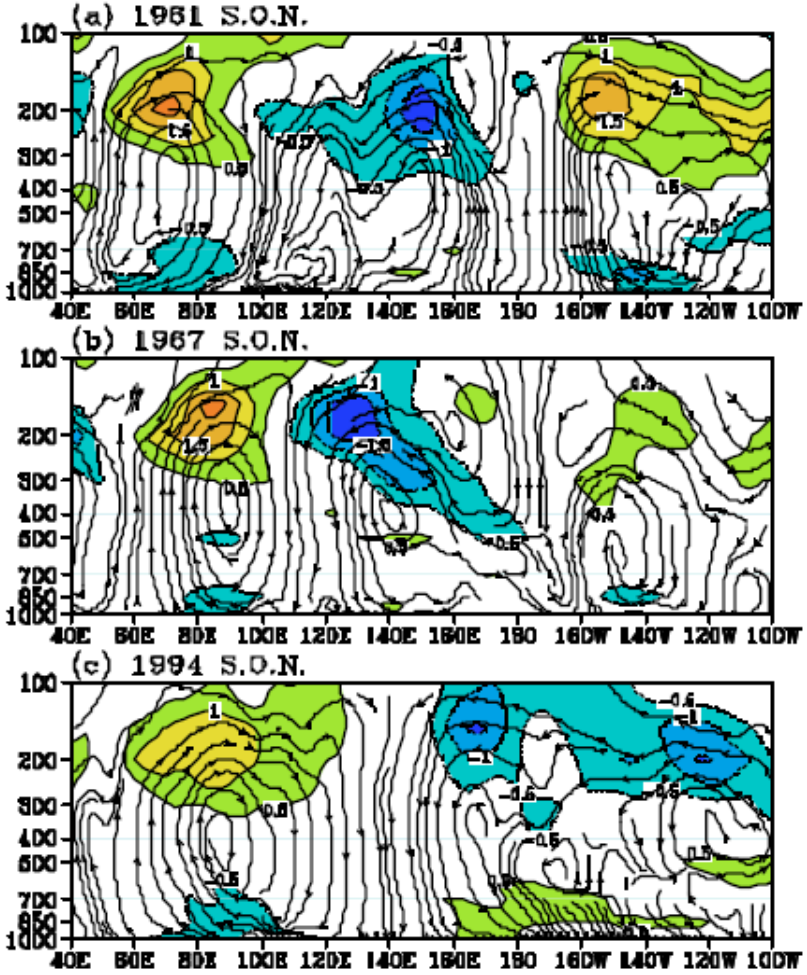

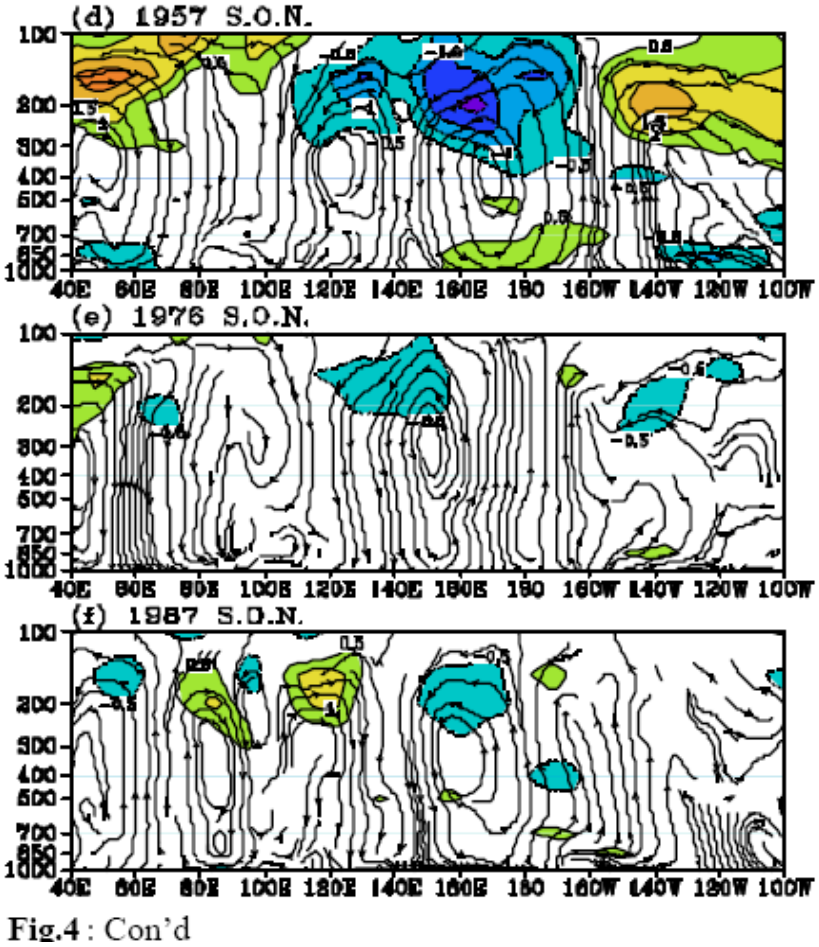

Fig.4 : Con'd

Fig. 4: (a-i) The height-longitude anomalous Walker circulation during September-October-November (SON), derived from the non-rotating zonal component of the velocity and the vertical velocity, during the years 1961, 1967, 1994, 1957, 1976, 1987, 1972, 1982, 1997 respectively. The colored contours in the background represent the divergent zonal winds ($m \cdot s^{-1}$); negative (positive) contours represent easterlies (westerlies)

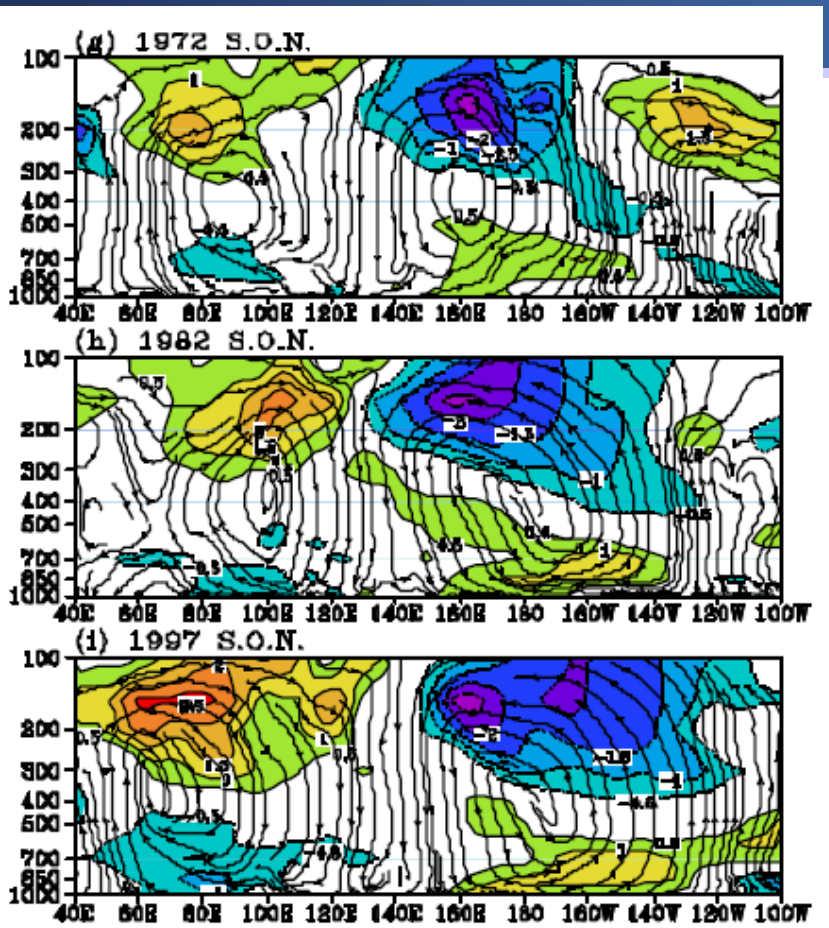

Fig. 4: (a-i) The height-longitude anomalous Walker circulation during September-October-November (SON), derived from the non-rotating zonal component of the velocity and the vertical velocity, during the years 1961, 1967, 1994, 1957, 1976, 1987, 1972, 1982, 1997 respectively. The colored contours in the background represent the divergent zonal winds ($m \cdot s^{-1}$); negative (positive) contours represent easterlies (westerlies)

Decadal Relationships (or the lack of it)

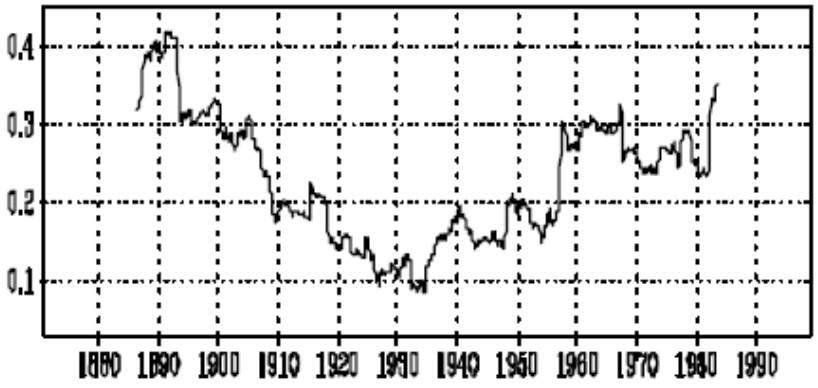

Fig. 6: The 31-year moving correlations between the normalized I_{IODM}, and normalized I_{NINO3} for the period from 1871 through 1998.

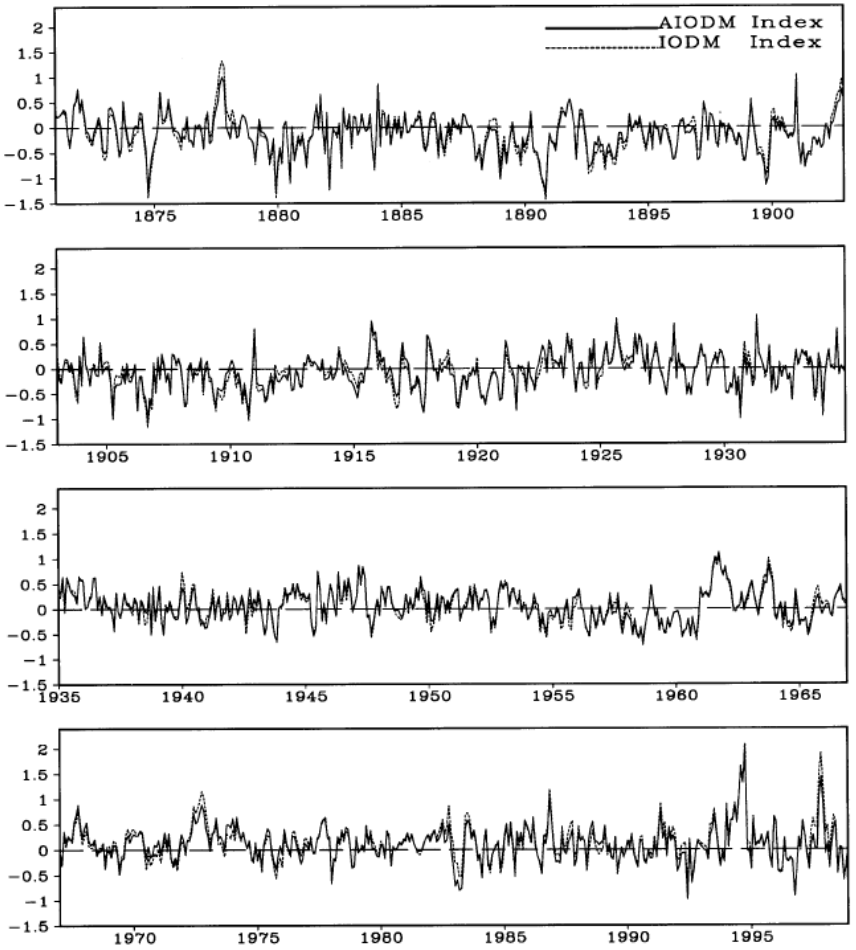

Fig. 7. (a) Time-series of the I_{IODM} (solid) and the I_{AIODM} (dashed), for the period from 1871 through 1998.

Table 3. The correlation matrix between I_{NINO3}, the NINO3 index and I_{IODM}, the IOD index. Each element represents the correlation between the time-series of I_{IODM} for the "i" month in 128 years and that of I_{NINO3} for the "j" month. The bold values are significant at 95% level.

		NINO3 INDEX											
MONTH		1	2	3	4	5	6	7	8	9	10	11	12
I	1	0.11	0.09	0.11	0.12	0.01	0.00	−0.02	−0.05	−0.03	0.04	0.00	0.01
O	2	0.00	0.06	0.06	0.15	0.11	0.14	0.05	0.06	0.05	0.10	0.10	0.12
D	3	−0.11	−0.08	−0.12	−0.07	−0.07	−0.01	−0.02	0.05	0.06	0.08	0.07	0.08
M	4	−0.10	−0.10	−0.12	−0.12	**−0.17**	**−0.19**	−0.16	−0.12	−0.10	−0.08	−0.06	−0.09
I	5	0.15	**0.18**	0.14	0.15	0.08	0.06	0.02	0.04	−0.03	0.01	0.02	0.03
	6	**0.18**	**0.20**	**0.20**	**0.26**	**0.24**	**0.23**	**0.22**	**0.23**	**0.18**	**0.18**	**0.19**	**0.18**
I	7	0.08	0.14	**0.17**	**0.32**	**0.37**	**0.43**	**0.33**	**0.34**	**0.28**	**0.26**	**0.26**	**0.29**
N	8	0.06	0.14	0.16	**0.27**	**0.27**	**0.34**	**0.31**	**0.35**	**0.30**	**0.30**	**0.33**	**0.33**
D	9	0.02	0.08	0.16	**0.27**	**0.34**	**0.37**	**0.36**	**0.40**	**0.40**	**0.42**	**0.43**	**0.44**
E	10	0.05	0.12	0.16	**0.25**	**0.32**	**0.37**	**0.38**	**0.43**	**0.43**	**0.46**	**0.48**	**0.48**
X	11	−0.04	0.05	0.10	**0.22**	**0.29**	**0.35**	**0.40**	**0.48**	**0.49**	**0.51**	**0.50**	**0.49**
	12	−0.11	−0.02	0.05	0.16	**0.19**	**0.30**	**0.30**	**0.32**	**0.31**	**0.34**	**0.36**	**0.34**

Table 4. The periodicities (in months) of the I_{NINO3}, I_{ATIO}, and the I_{IODM}. I_{NINO3} is the NINO3 index, I_{ATIO} is the mean SSTA, averaged over the whole tropical Indian Ocean, and I_{IODM} is the IOD index.

Confidence Level (α)	$\alpha \geq 95\%$	$95\% > \alpha \geq 90\%$
Periods in I_{NINO3}	**43.5**; **34.5**; 17.9	16.4; 13.5
Periods in I_{ATIO}	**43.5**	**58.8**
Periods in I_{IODM}	**62.5**	125.0; 25.6; **10.1**

The independent coupling processes in the Indian Ocean

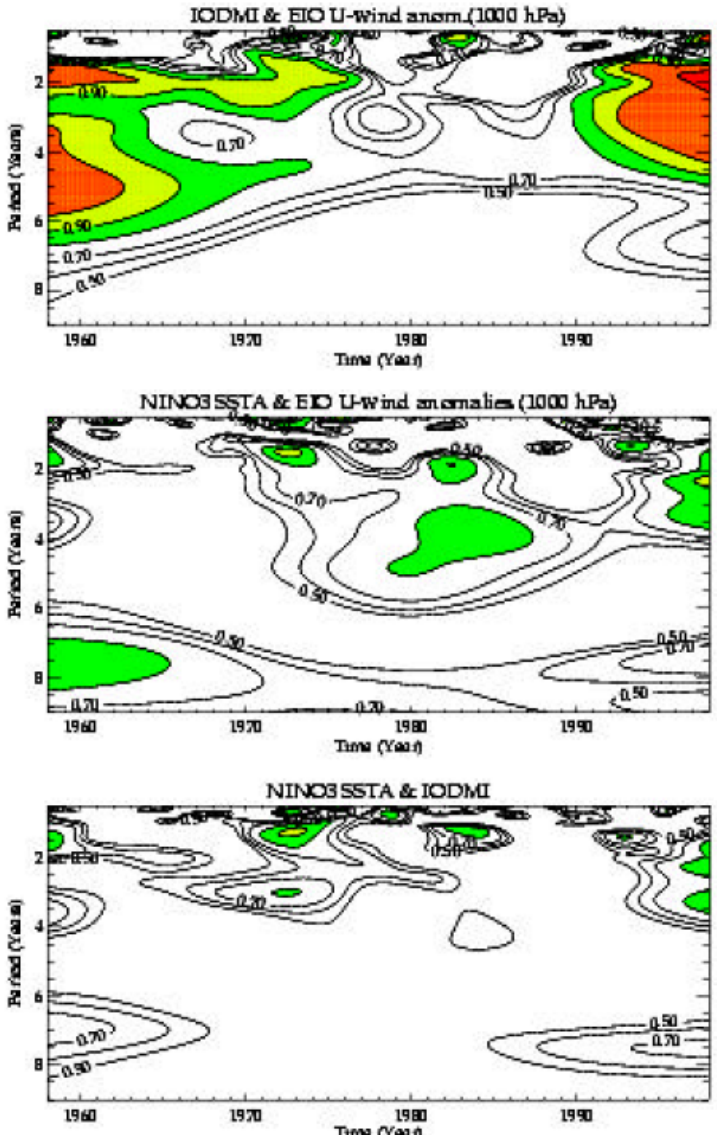

Fig. 8: (a) The wave coherency for the period from 1958-1997 between (a) the I_{IODM} time series and the EIOZWA (b) I_{NINO3} and the EIOZWA (c) I_{IODM} and I_{NINO3}. Values greater than 0.82 (significant at 95% confidence level, obtained from 1000 Monte-Carlo simulations of the white noise) are shaded.

The Abrupt termination of the Indian Ocean Dipole event due to Intraseasonal Dsturbances

Introduction

- Intraseasonal Disturbaces (ISD) known as trigger for ENSO (Luther et al., 1995, Kessler et al., 1995).
- Termination of the 1997 El Niño by the intraseasonal easterly winds due to ISD (Takayabu et al., 1999).
- Northward propagation of Indian summer monsoon (many papers).
- *Killer of the IOD events?*

Data

- Monthly GISST (1958-1982)
- Weekly OISST (1982-1997)
- 3-day rainfall from TRMM (1998-2003)
- Merged SSH data from Aviso, France (1993-2003).
- Surface Zonal winds NCEP/NCAR (1958-2003), ERA (1958-2001).
- Satellite derived QUICKSCAT winds (2000-2003).
- GPCP rainfall (1979-2003)
- Lanzcos Bandpass filter (20~100days).

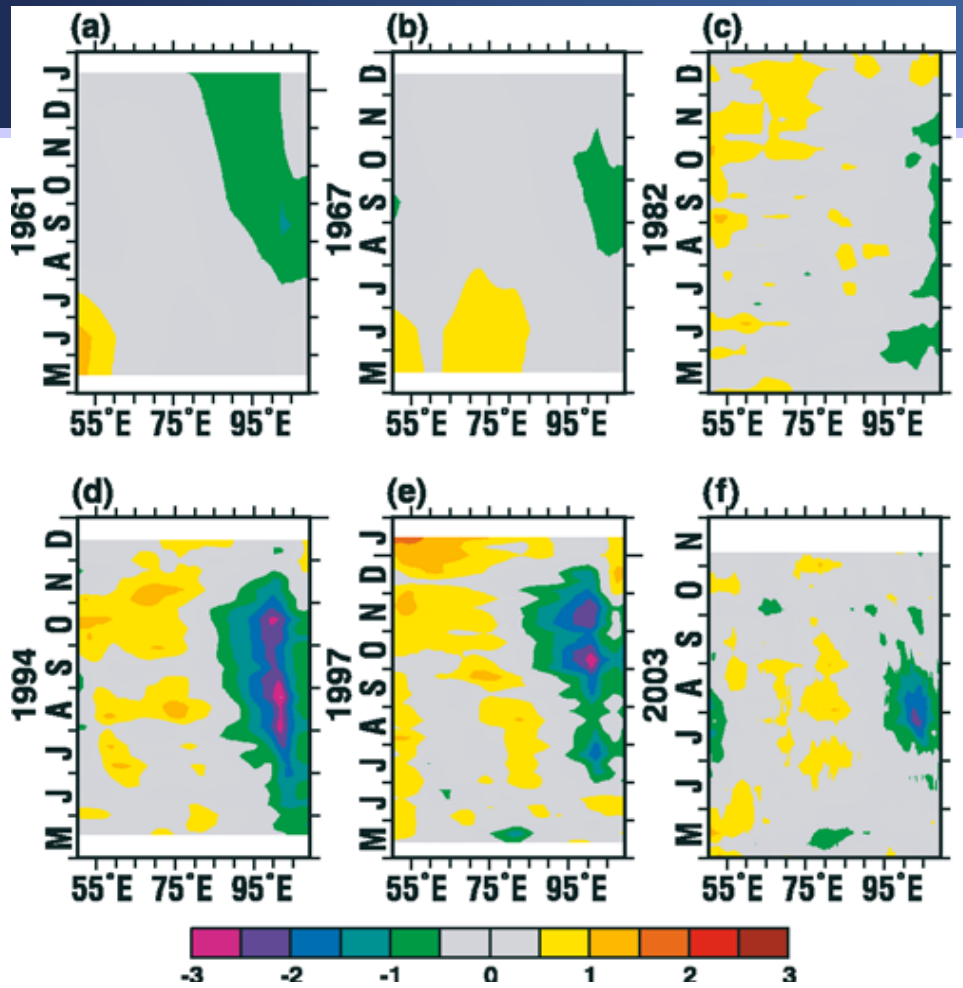

Figure 1. SST anomalies (deg. C) averaged between 10S-Eq in the tropical Indian Ocean for (a) 1961, (b) 1967, (c) 1982, (d) 1994, (e) 1997 and (f) 2003 IOD events. Monthly GISST data is used for (a) and (b), weekly OI SST is used for (c), (d) and (e) and 3-day SST from TMI onboard TRMM is used for (f).

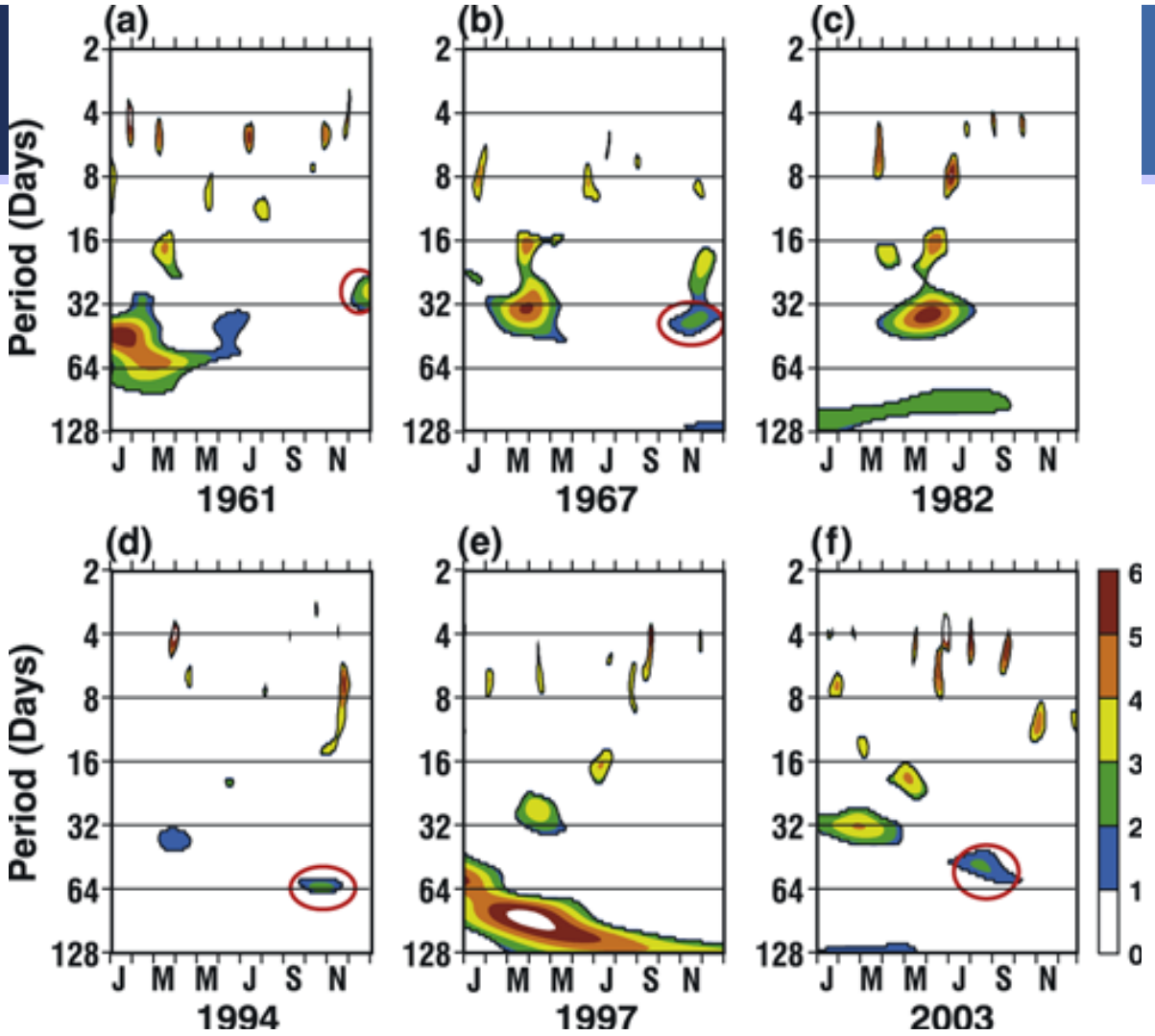

Figure 2. Wavelet spectrum of equatorial daily zonal wind anomalies for 1961, 1967, 1982, 1994, 1997 and 2003 IOD events. Daily zonal winds from NCEP/NCAR reanalysis are used. The wavelet spectrum is normalized with the global wavelet spectrum and normalized spectrum is plotted only if the spectrum is significant at 95% confidence limit. Ellipses (Thick line) show the regions of significant 30–60 day oscillations in zonal wind prior to the termination of IOD events.

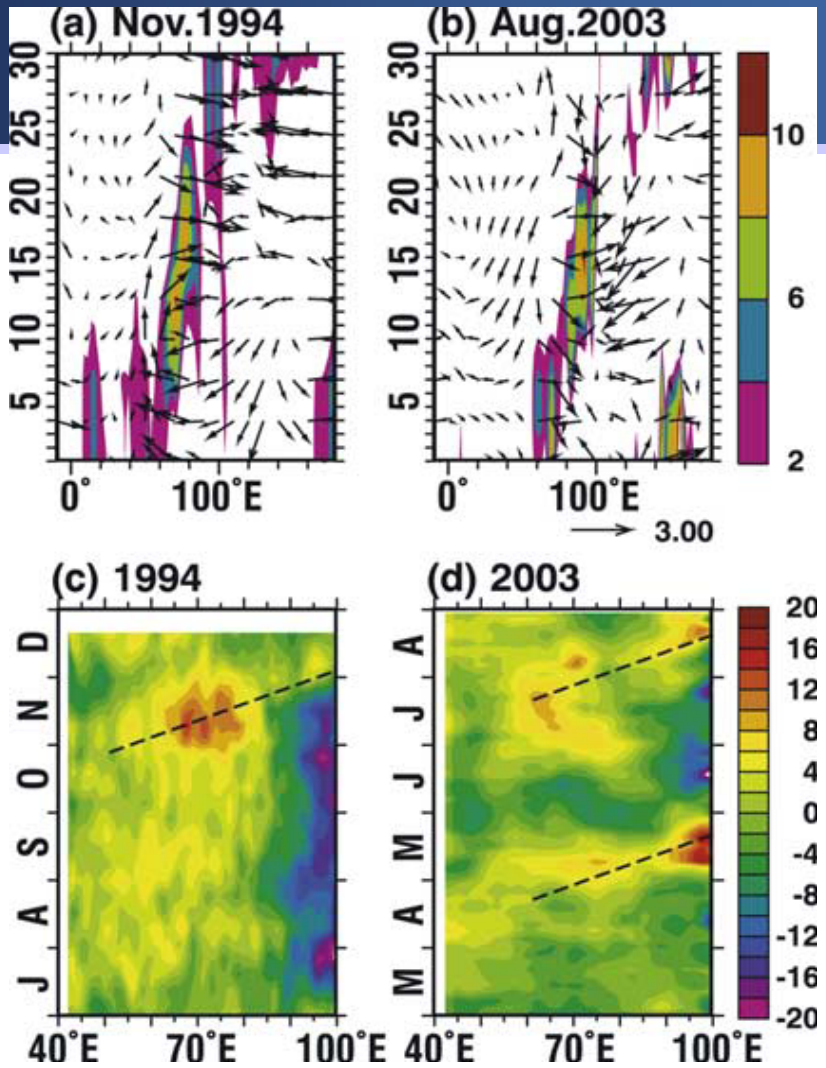

Figure 3. 20–90 day filtered anomalies of rain (shading, mm/day) and winds (vectors, m/sec) averaged between 10S–10N for (a) 1994 and (b) 2003 IOD events. SSH anomalies (cm) for (c) 1994 and (d) 2003 IOD events from merged SSH dataset. GPCP pentad rainfall is used for (a) and TMI rainfall is used for (b) Path of propagation of downwelling Kelvin-wave is shown with dashed line.

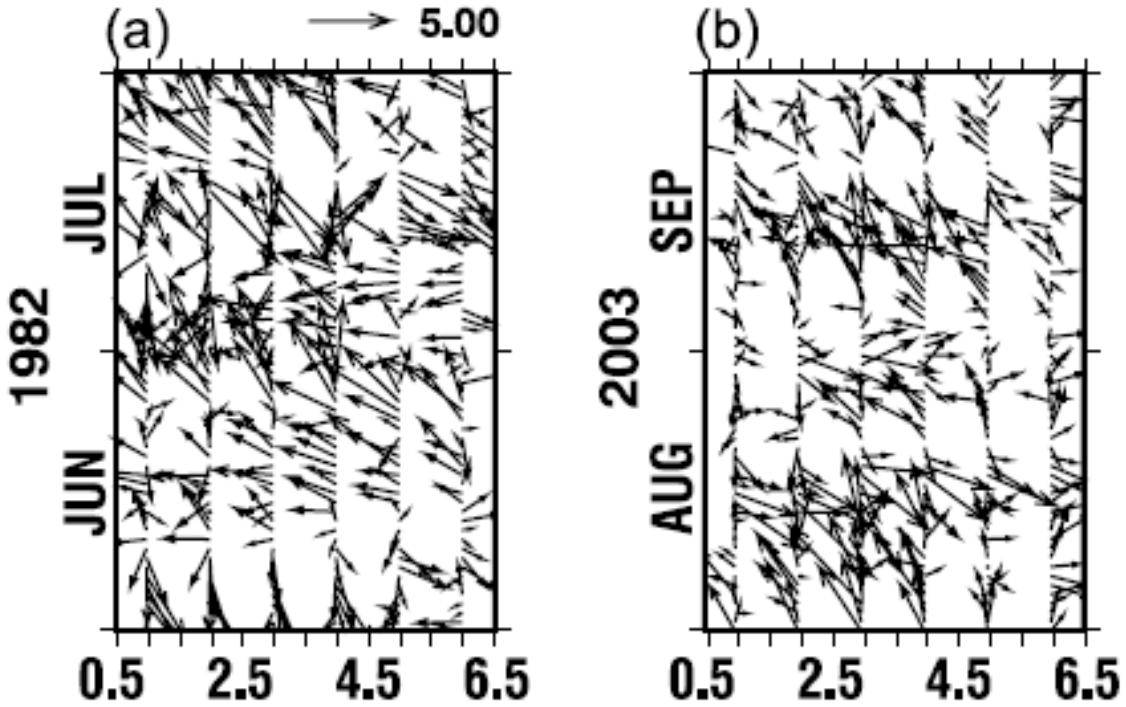

Figure 4. Daily wind vectors (m/sec) averaged in different boxes along the coast of Sumatra and Java for (a) 1982 and (b) 2003 IOD events. Units along the x-axis are box numbers 1. (95–100°E, 2°S-Eq.), 2. (95–100°E, 2°–4°S), 3. (97–102°E, 4°–6°S), 4. (99–104°E, 6°–8°S), 5. (104–108°E, 8°–10°S), and 6. (108–112°E, 8°–10°S).


Center in Busan APEC Cimate Center in Busan APEC Cimate Center in Busan APEC Cimate Center in Busan APEC Cimate Center in Busan APEC Cimate Center in Busan APEC Cimate Center in Busan APEC Cimate Center in Busan APEC Cimate Center in Busan
야경투시도
Variability of the Indian Ocean Dipole
in a 10,000 year CGCM simulation
주경투시도

IOD variability

- The primary significant power at biennial peak (Saji et al, 1999), followed by a quasi-pentadal peak (Ashok et al., 2003a; *from GISST 1871-1998*).
- *Also, significant at 90% confidence level is a peak at 125-months (Ashok et al. 2003a; from GISST 1871-1998*).

Slower frequency impacts/modulations

- Decadal modulation of the IOD frequency, and its role in weakening of ENSO-Indian monsoon relationship (Ashok et al., 2001).
- Weakening of the El Nino-Southern Oscillation period in recent decade (Behera et al., 2003).
- Decadal and centennial modulation of the IOD SST (Abram et al., 2003).

Datasets

- GISST (Rayner et al., 1996)
- SODA Z20 depth (Carton et al., 2000)

from 1950-1999

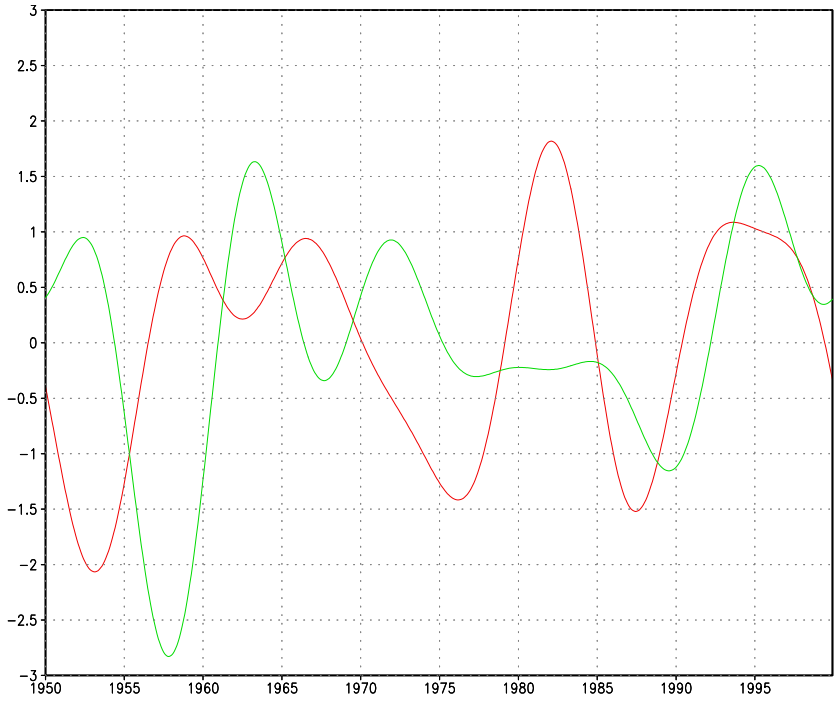

Decadal signals (8-25 years) of IODMI (green) and NINO3 SSTA from GISST

Observed decadal (8–25 years) partial correlations
between IODMI and anomalies of Z20

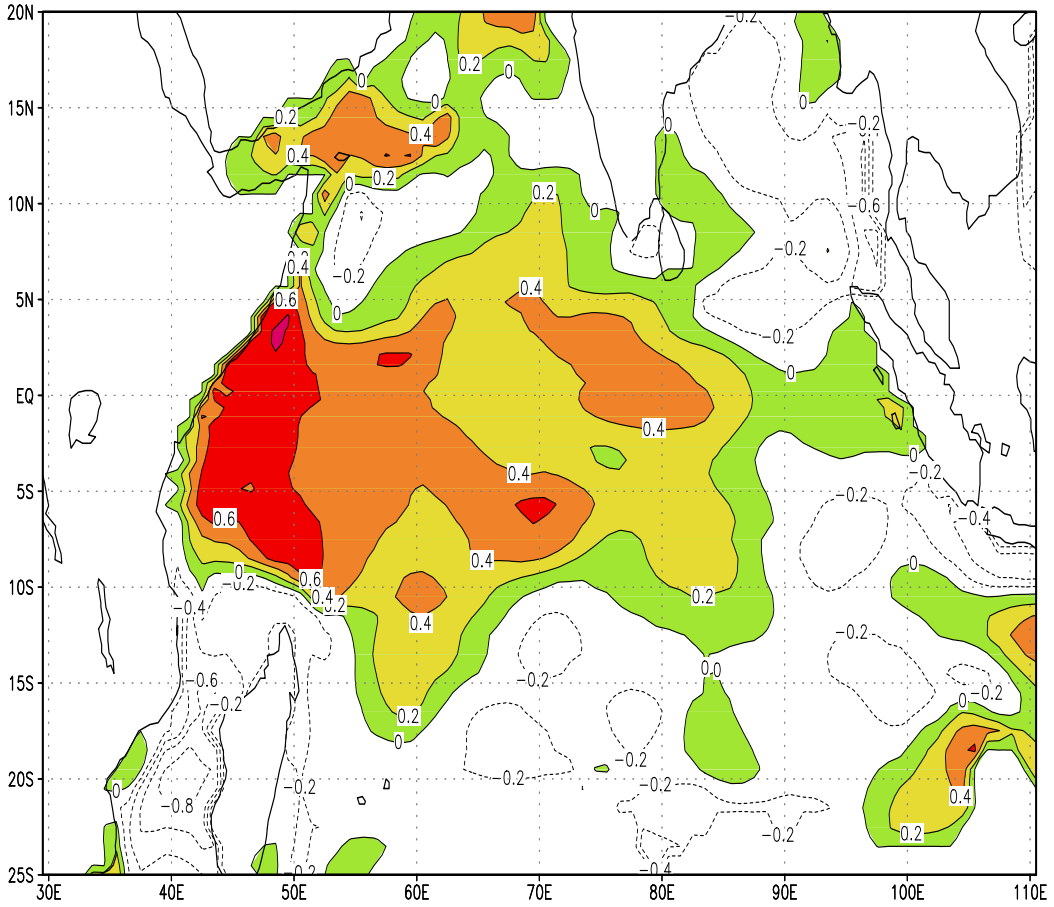

Brief description of GFDL coupled model:

AGCM: 9 vertical levels, horizontal resolution R15. Seasonally-varying insolation.
OGCM: 12 vertical levels, horizontal grid of approx 4.5˚ (lat) by 3.75˚ (lon).
Atm-ocean interaction once a day (heat, water and momentum flux exchanges). Simple sea-ice model also included. Land component: uses bucket model. Flux corrections incorporated. Time integrations (10,000 yrs); most of the work shown here is based on the analysis of outputs between years 4001-5000.

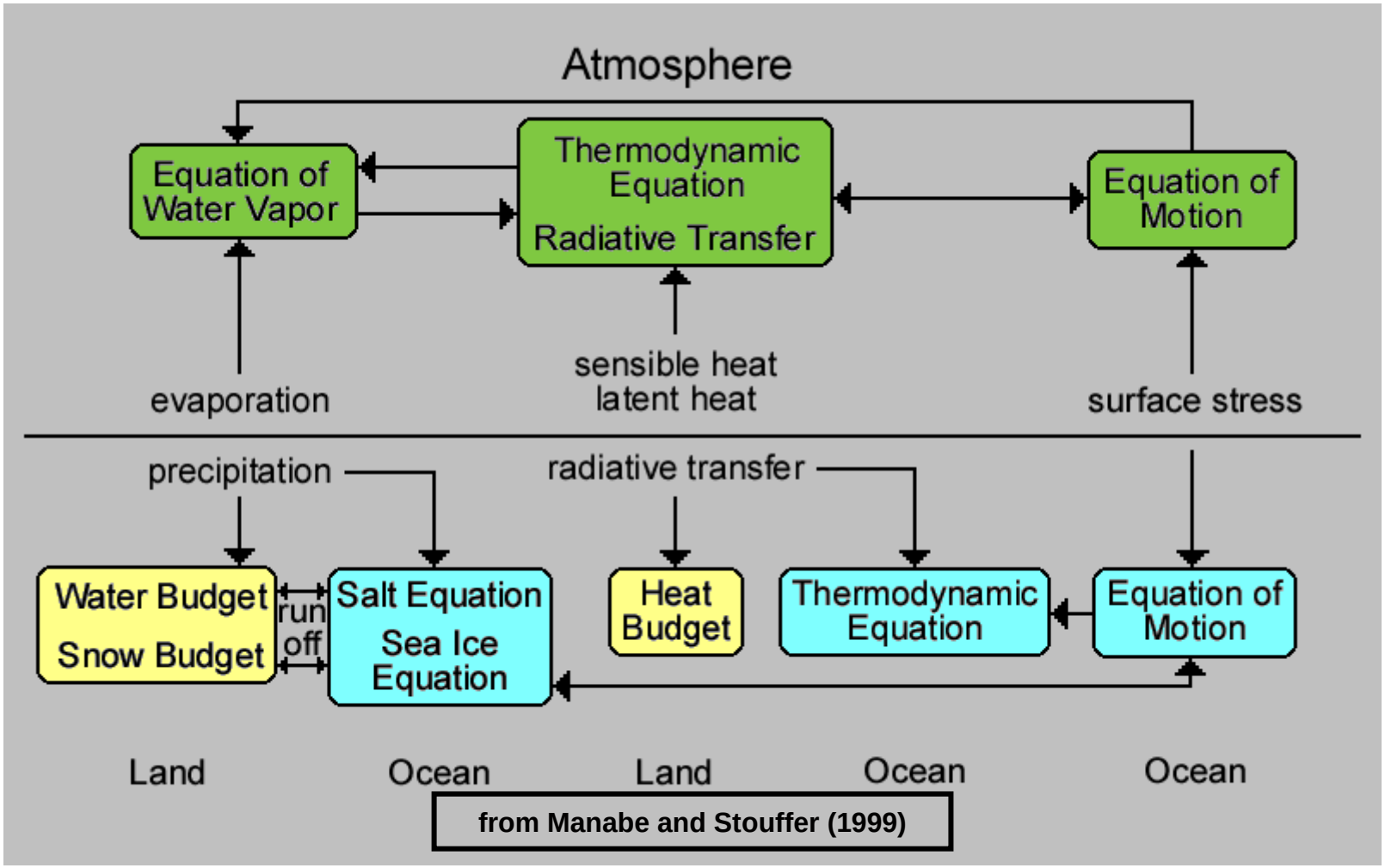

from Manabe and Stouffer (1999)

EOF1(11.1%); D100-SON SSTA

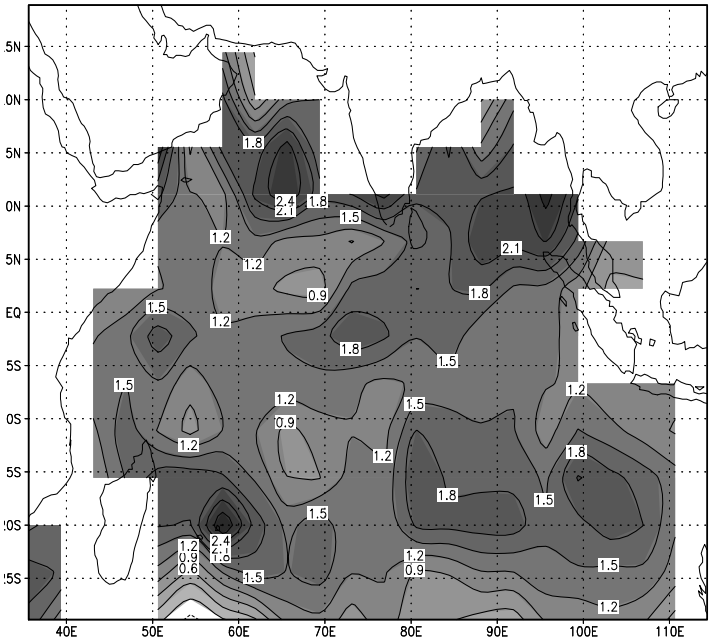

EOF2(10.1%); D100-SON SSTA

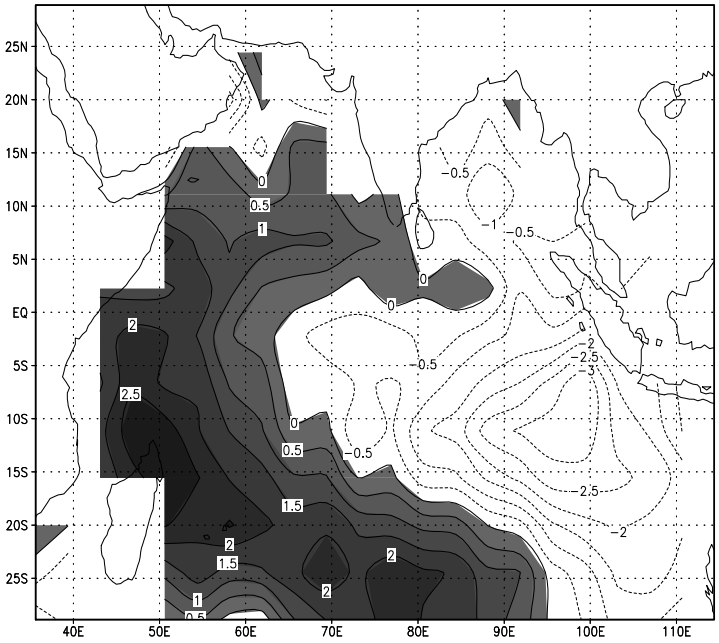

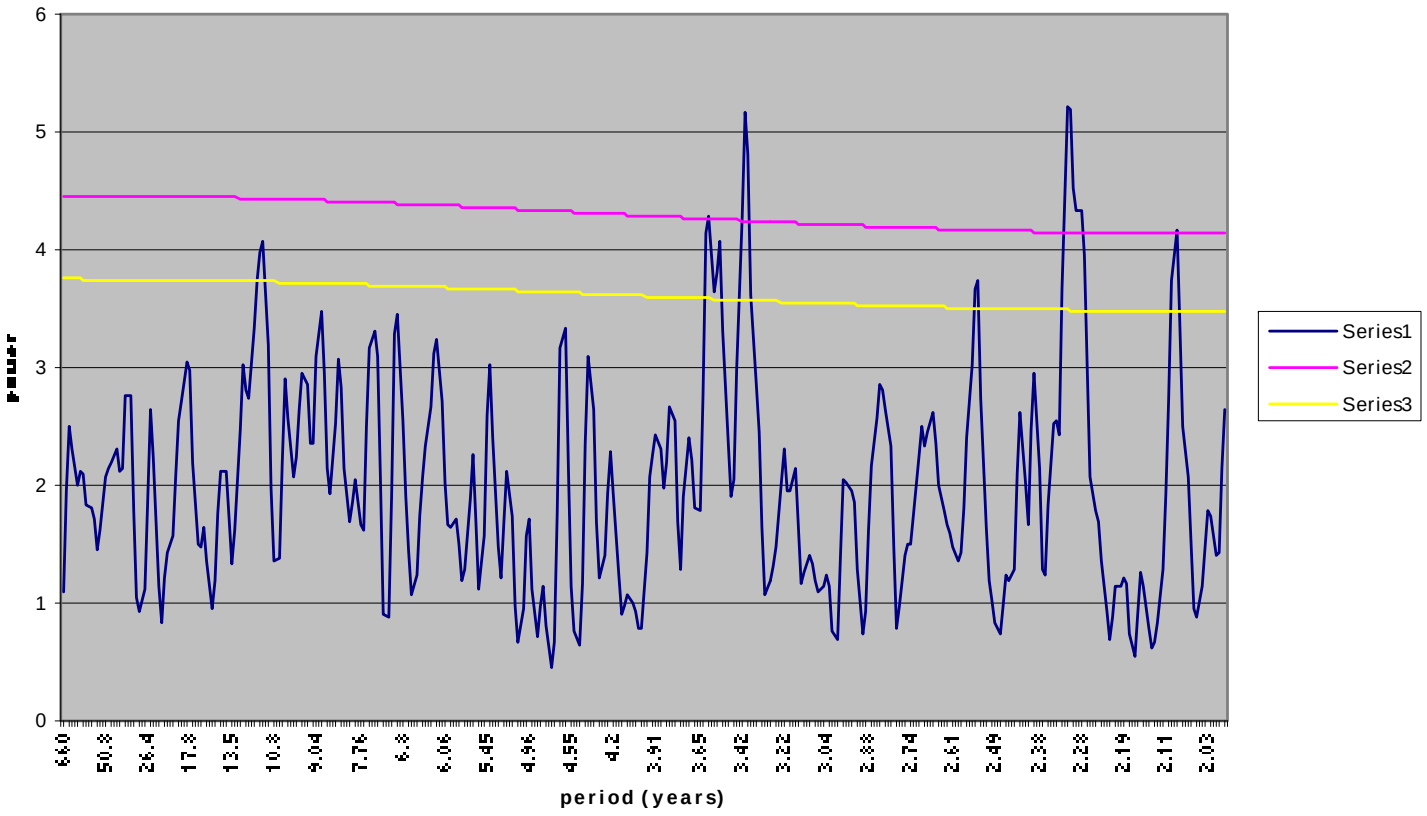
IODMI power (E1000)
power
period (years)
66.0
50.8
26.4
17.8
13.5
10.8
9.04
7.76
6.8
6.06
5.45
4.96
4.55
4.2
3.91
3.65
3.42
3.22
3.04
2.88
2.74
2.61
2.49
2.38
2.28
2.19
2.11
2.02
0
1
2
3
4
5
6
Series1
Series2
Series3

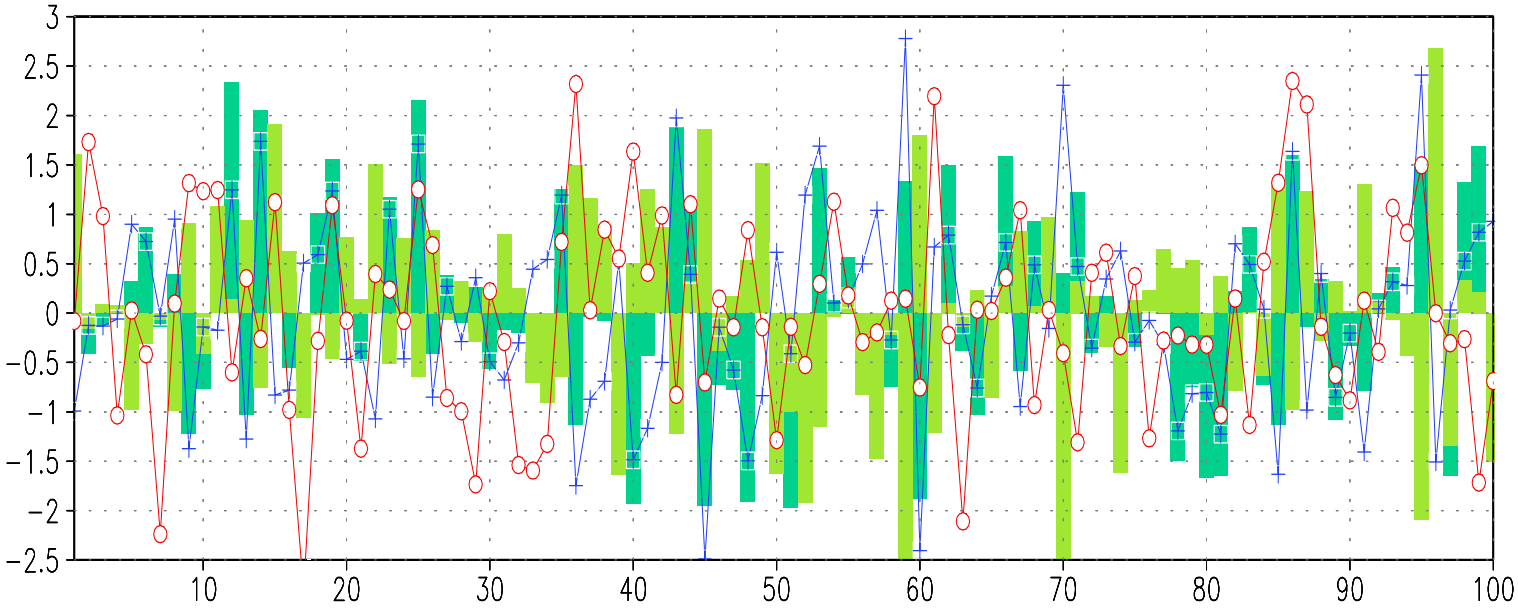

Time series of SON anomalies during J100: IODMI (Blue line), NINO index (Red line),
Western Box (Aqua Bar), and Eastern Box (Yellow Bar)
Western Box (15S−10N,40E−60E), and Eastern Box (15S−Equator,90E−110E), NINO index (7S−7N, 173E−120W)

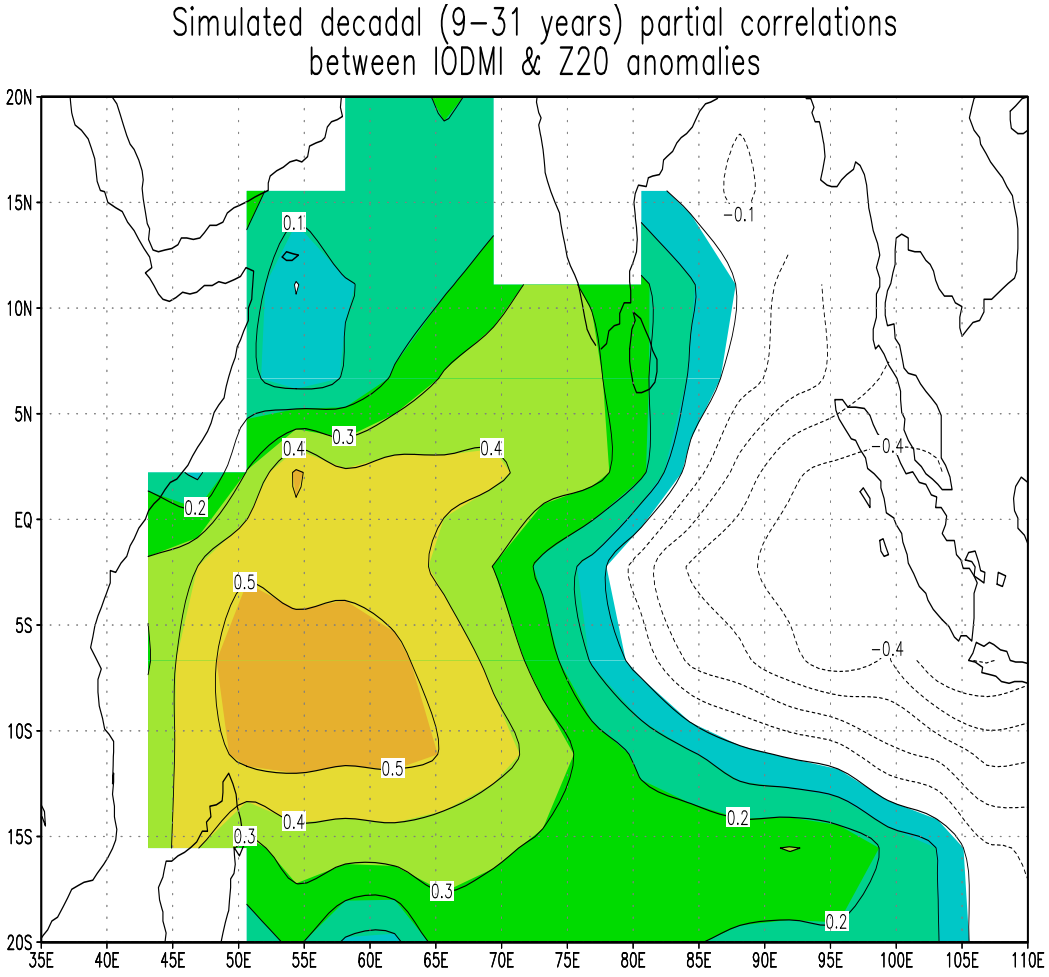
Simulated decadal (9–31 years) partial correlations
between IODMI & Z20 anomalies
20N
15N
10N
5N
EQ
5S
10S
15S
20S
35E
40E
45E
50E
55E
60E
65E
70E
75E
80E
85E
90E
95E
100E
105E
110E
0.1
−0.1
0.4
0.3
0.4
−0.4
0.2
0.5
−0.4
0.5
0.4
0.2
0.3
0.3
0.2

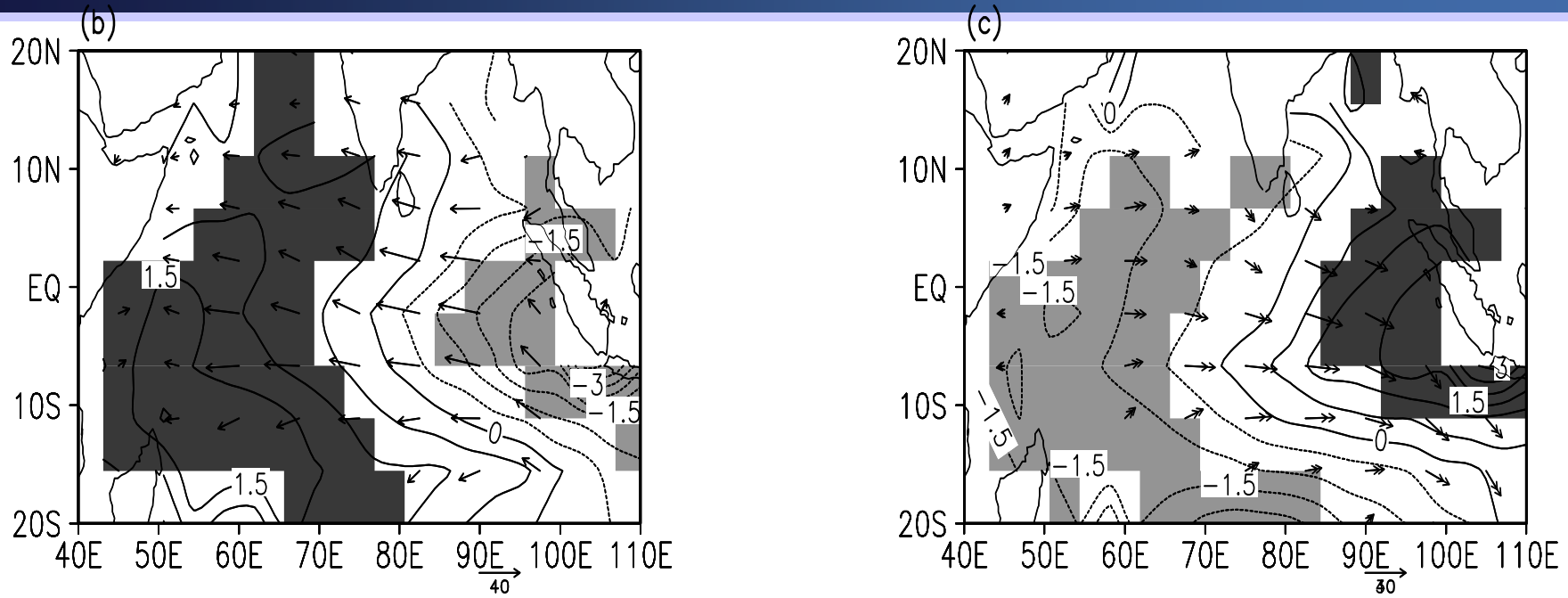

Simulated decadal (8-31 year signals) (b) composite D20 anomalies (cm) during 1st year of the cycle; in contours, and surface winds (cm.s-1) (c) same as b, but in 6th year. Shaded values are significant at 90% confidence level from 2-tailed t-test. The whole process similar to that of the interannual IOD [Saji et al., 1999; Rao et al., 2002] except for the much longer timescale. This situation reminds us of such similarity between delayed oscillator theory for the interannual ENSO [Schopf and Suarez, 1988] and that for the decadal ENSO [Knutson and Manabe, 1998]. However, the phase speed (of about 0.08 m/sat 10ºS) of simulated decadal Rossby waves is smaller than the theoretical prediction of 0.18 m/s. This may be due to their coupling with the overlying atmosphere, as suggested by White et al [2003] in the context of slower tropical Pacific decadal waves.

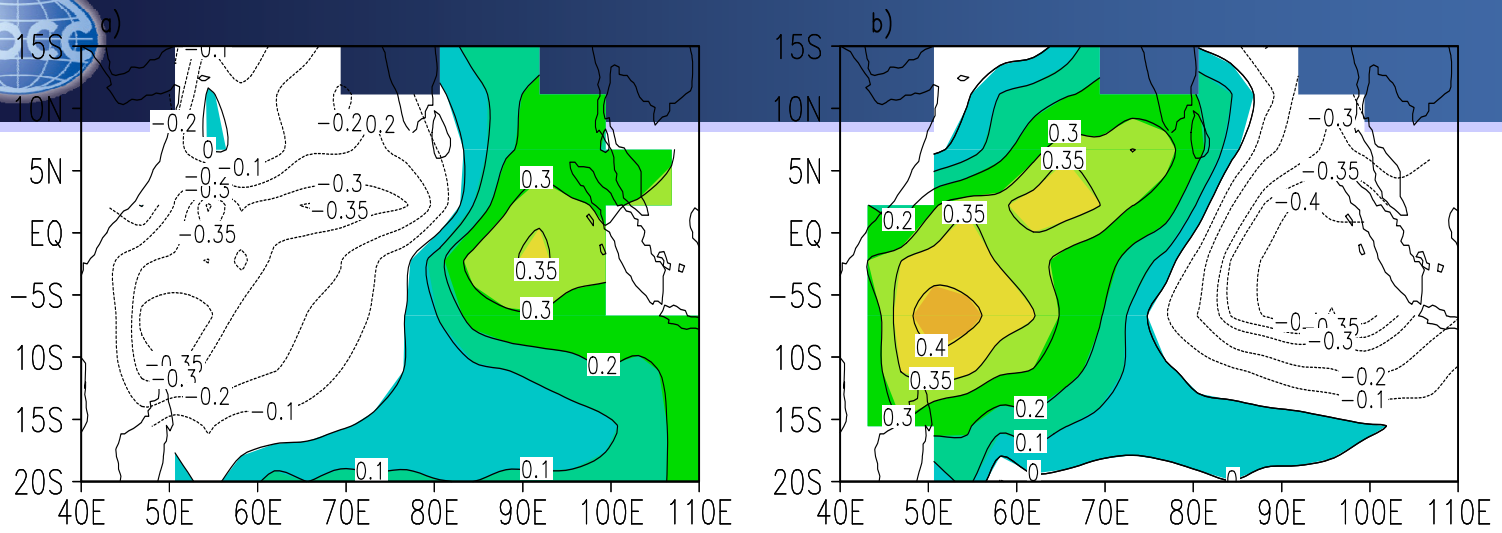

Correlations between simulated decadal (8-31 year signals) SON D20 anomalies with JJA Webster-Young index with the latter leading by 5 years (a) and for the same year (b).

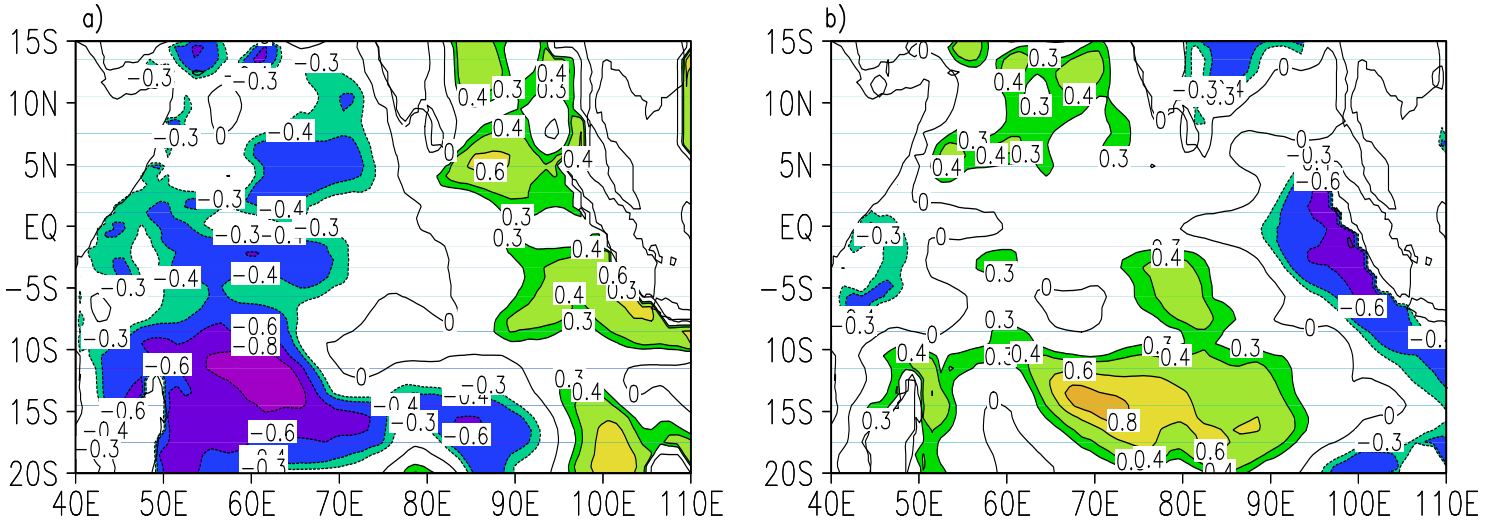

Same as above, but for decadal (8-25 year signals) correlations between SON SODA-derived D20 anomalies and NCEP derived decadal JJA W-Y index.

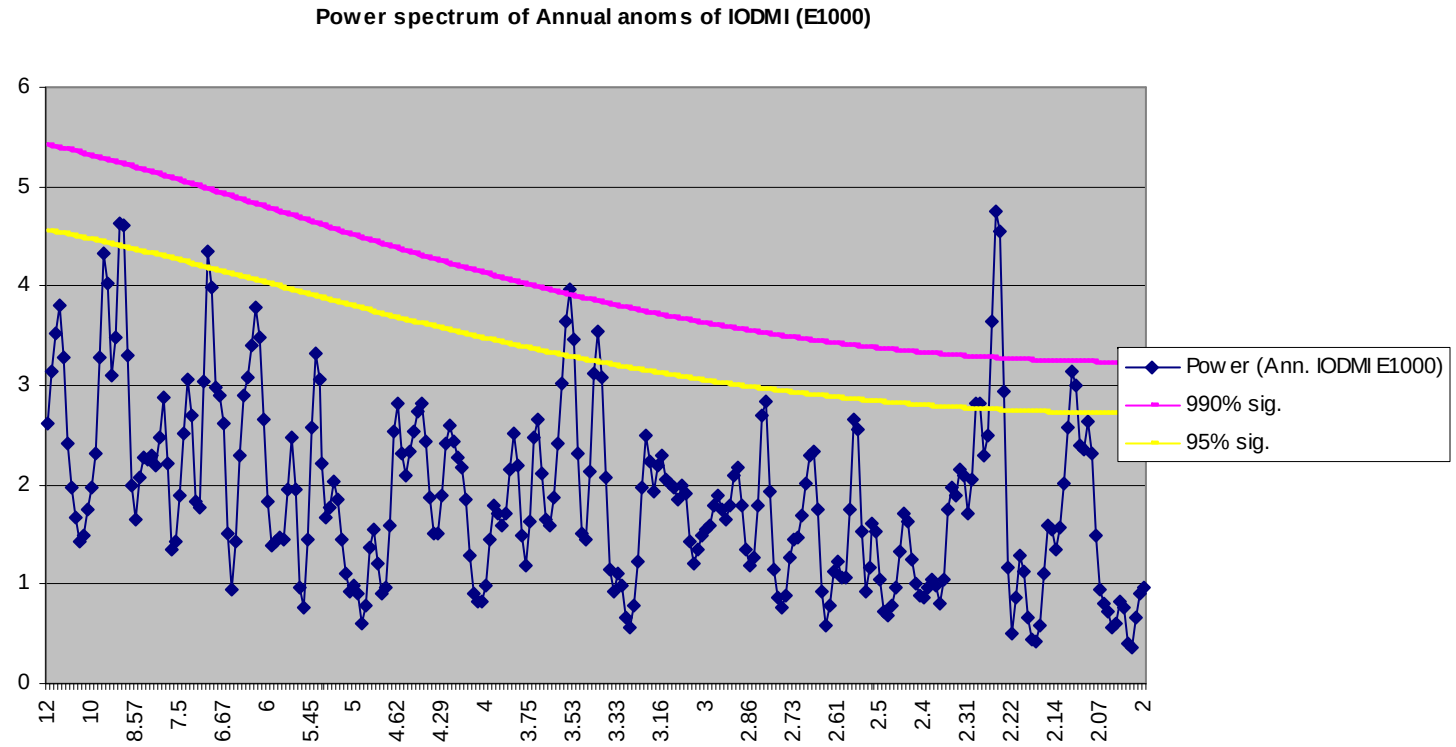
Power spectrum of Annual anoms of IODMI (E1000)
6
5
4
3
2
1
0
12
10
8.57
7.5
6.67
6
5.45
5
4.62
4.29
4
3.75
3.53
3.33
3.16
3
2.86
2.73
2.61
2.5
2.4
2.31
2.22
2.14
2.07
2
Power (Ann. IODMI E1000)
990% sig.
95% sig.

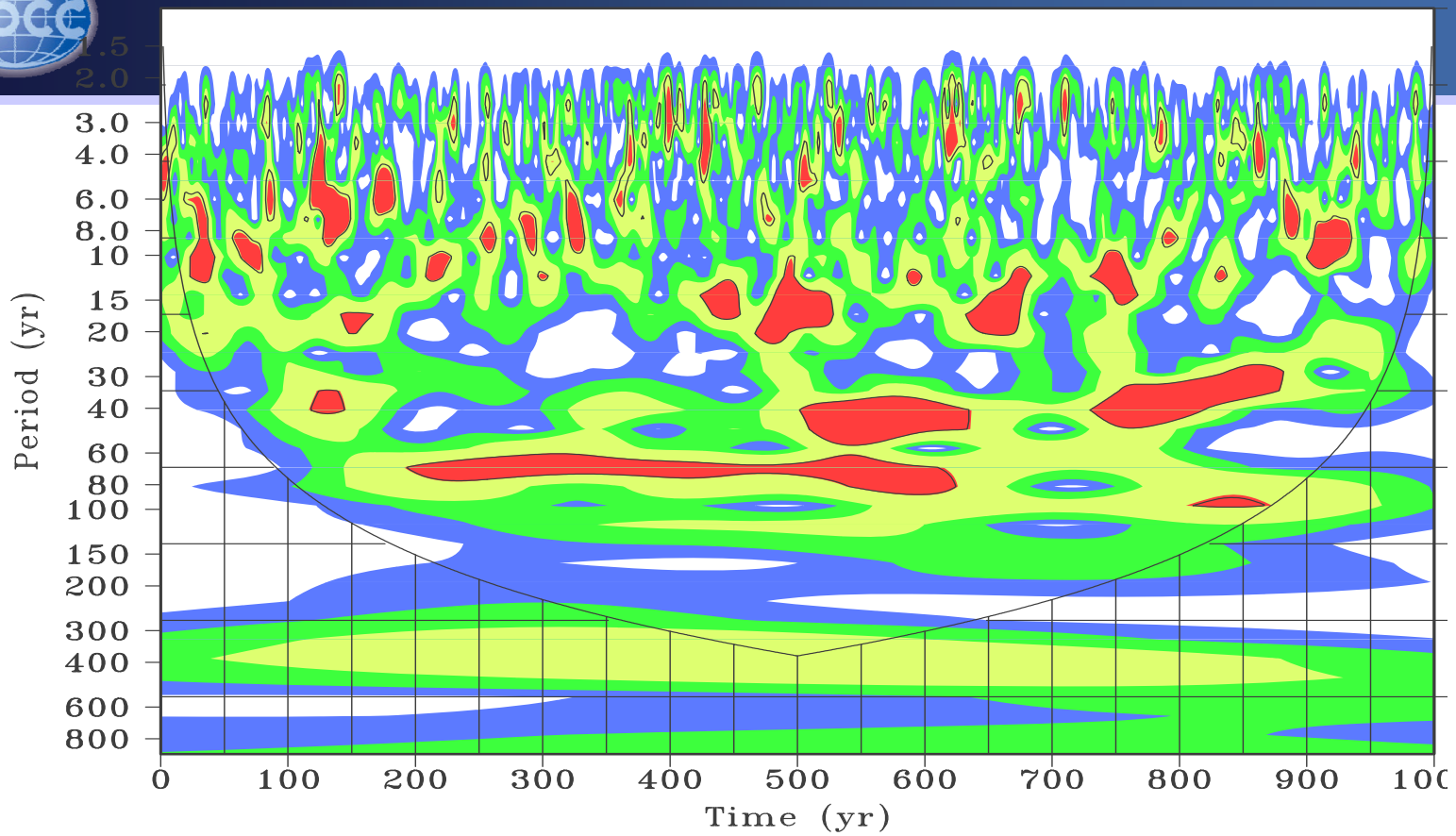

Wavelet spectrum of the simulated annual IODMI. Significant values (at 95% confidence level from red noise spectrum) are circumscribed by a thick line. Hatched lines indicate regions with variance reduced due to padding. The correlation between the scale-averaged variance of 2-8 (5-8) year band with that of 8-32 years is 0.23 (0.34), which is significant at 99.9% confidence level.

Tozuka et al. [personal communication, 2004] have recently suggested that decadal asymmetric occurrence of positive and negative IOD events may lead us to a decadal IOD-like picture because of linear statistical analysis methods. Such simulated association between the asymmetric interannual fluctuations of SST over the western pole of the IOD, and its decadal component is presented in next slide as an example. The prospective role of the occurrence of asymmetric interannual events in such "*decadal regime shifts*" is a topic that has to be explored further.

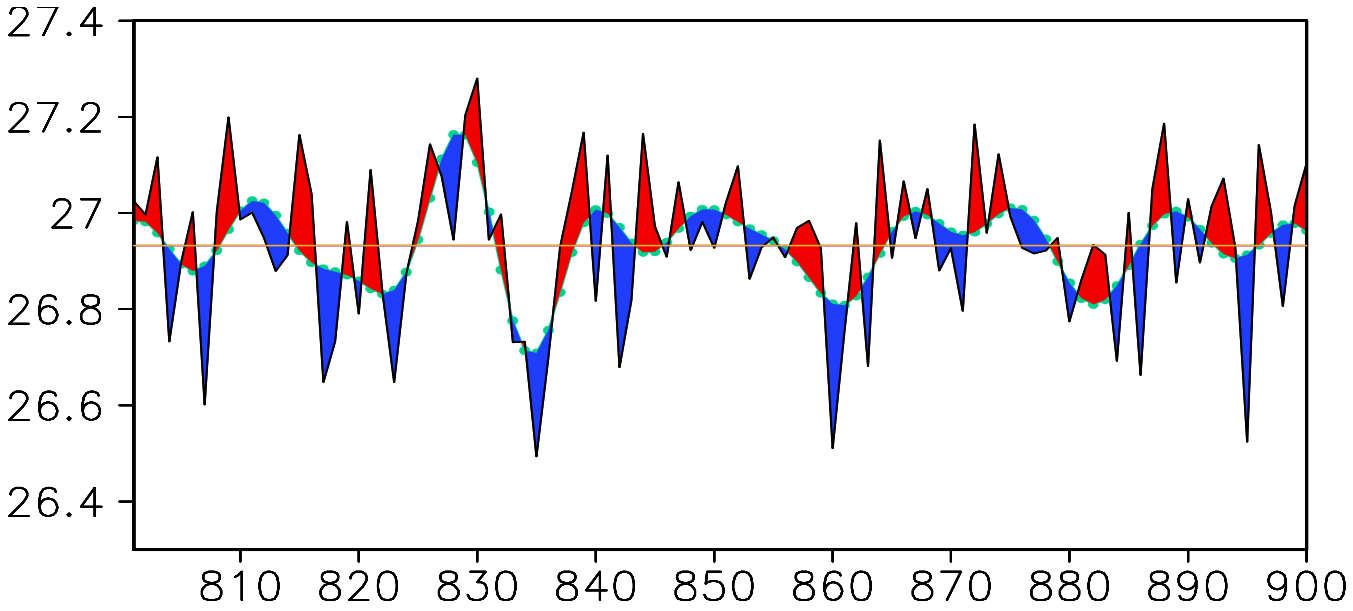

Interannual fluctuations of SST averaged over the western pole of the IOD (black line), and decadal (8-31 years) fluctuations over the same region (circles). Straight line is the time-average over 1000 years. Values from years 801 to 900 are shown as example. Methodology similar to Fig. 1a of Federov and Philander [2000] except that apart from the removal of seasonal cycle and high frequency components, multidecadal and centennial signals also have been removed.

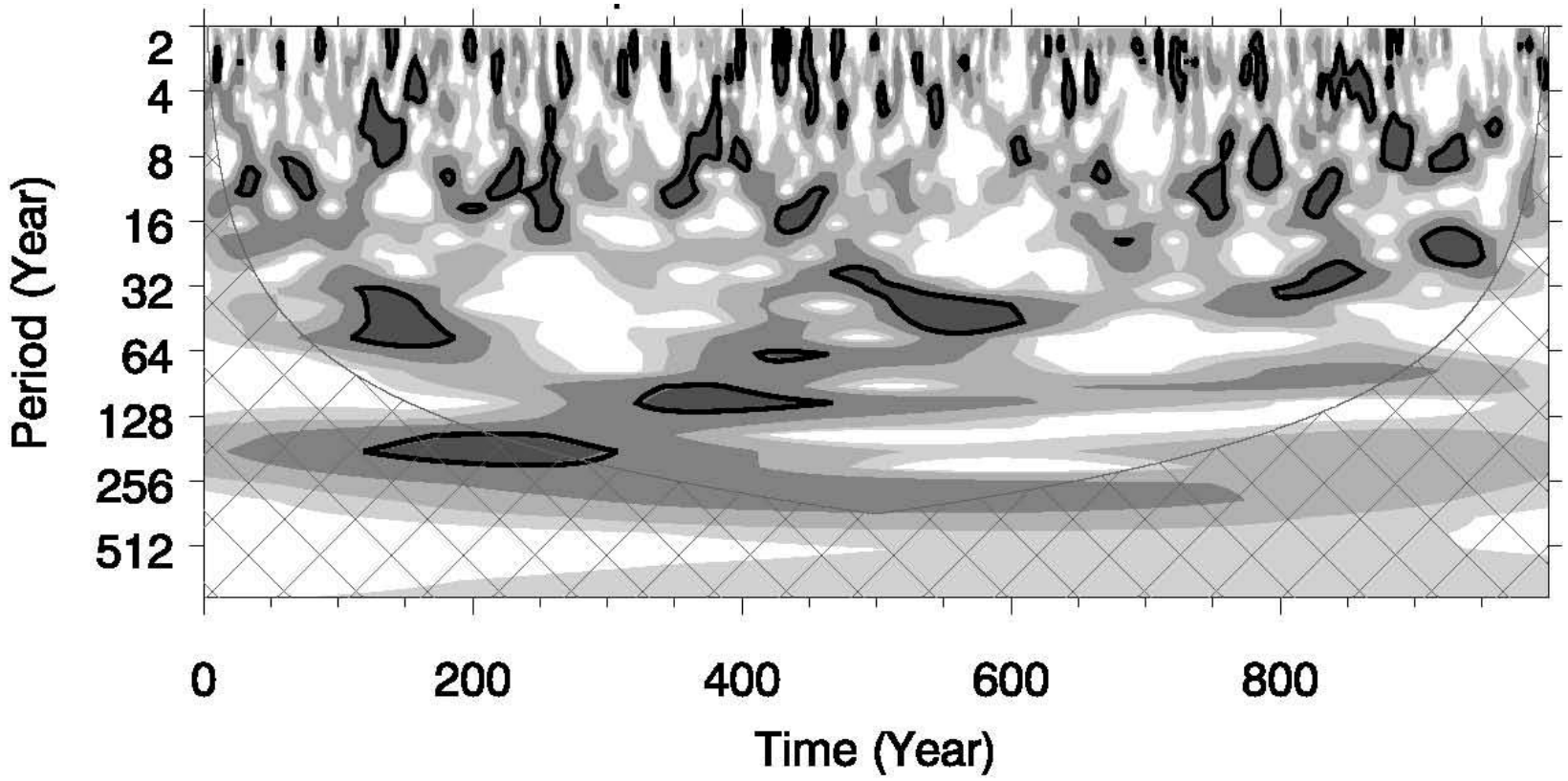
Period (Year)
2
4
8
16
32
64
128
256
512
0
200
400
600
800
Time (Year)

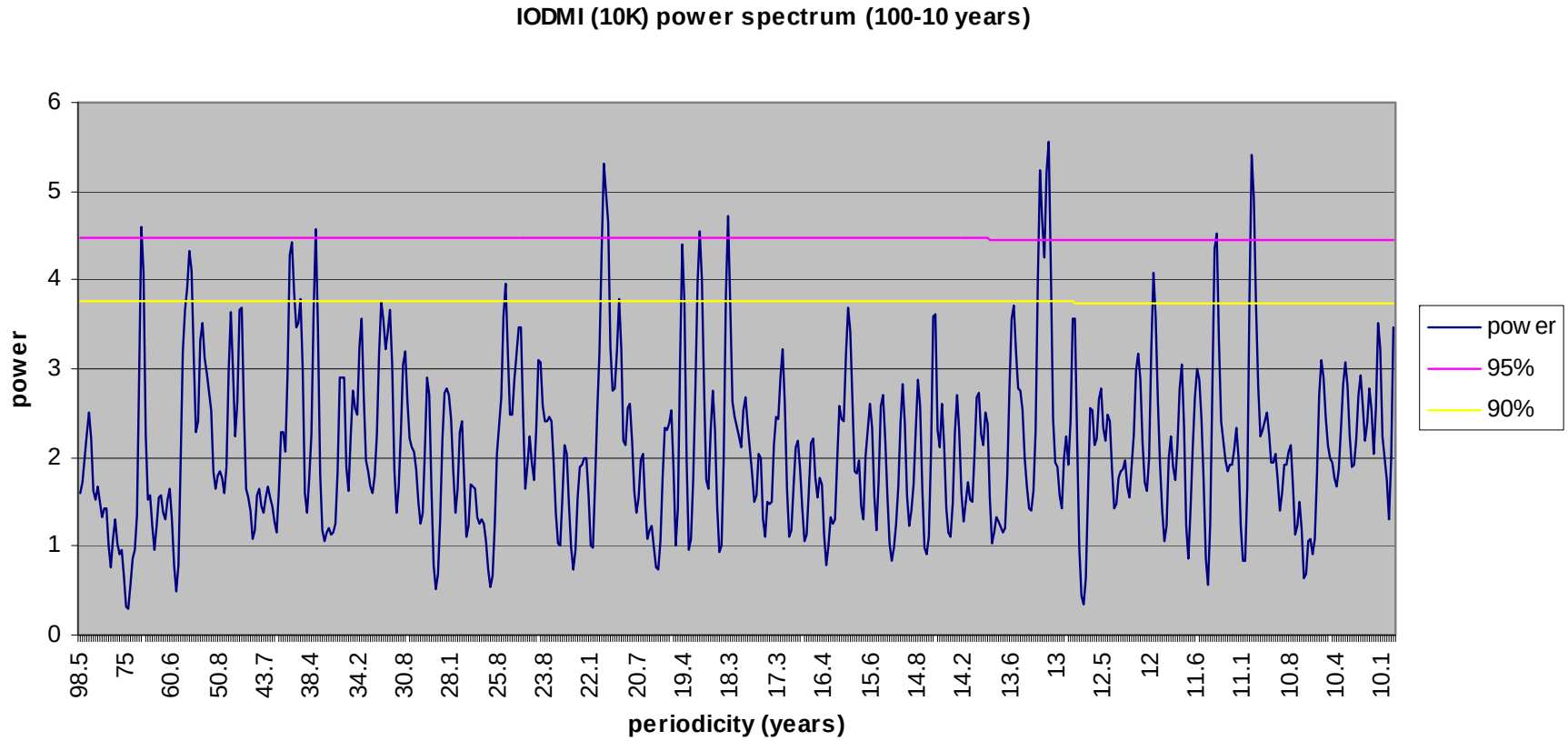
IODMI (10K) power spectrum (100-10 years)
power
periodicity (years)
0
1
2
3
4
5
6
98.5
75
60.6
50.8
43.7
38.4
34.2
30.8
28.1
25.8
23.8
22.1
20.7
19.4
18.3
17.3
16.4
15.6
14.8
14.2
13.6
13
12.5
12
11.6
11.1
10.8
10.4
10.1
power
95%
90%

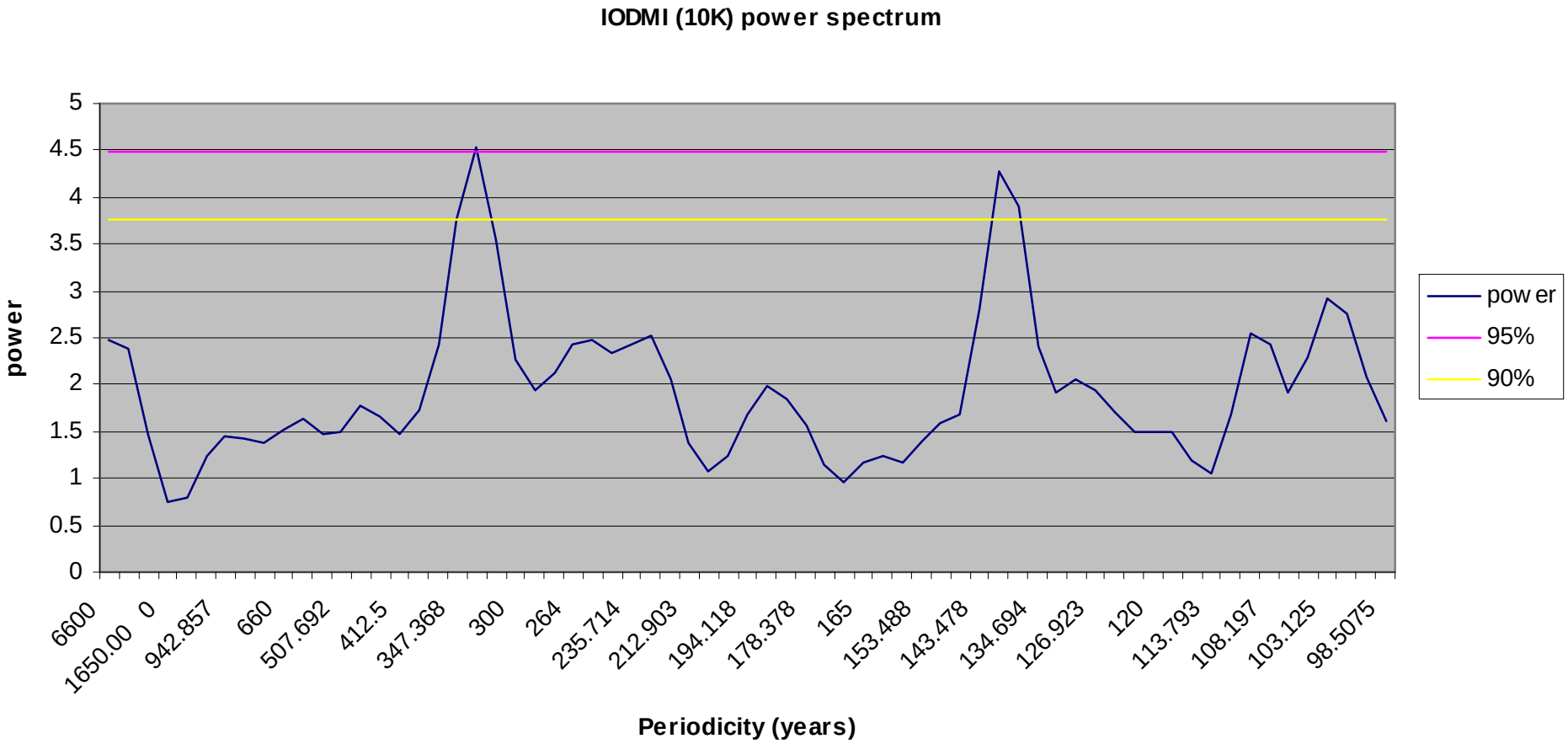
IODMI (10K) power spectrum
power
5
4.5
4
3.5
3
2.5
2
1.5
1
0.5
0
6600
1650.00
0
942.857
660
507.692
412.5
347.368
300
264
235.714
212.903
194.118
178.378
165
153.488
143.478
134.694
126.923
120
113.793
108.197
103.125
98.5075
Periodicity (years)
power
95%
90%

Simulated centennial (315–345 years) correlations between IODMI & Z20 anomalies

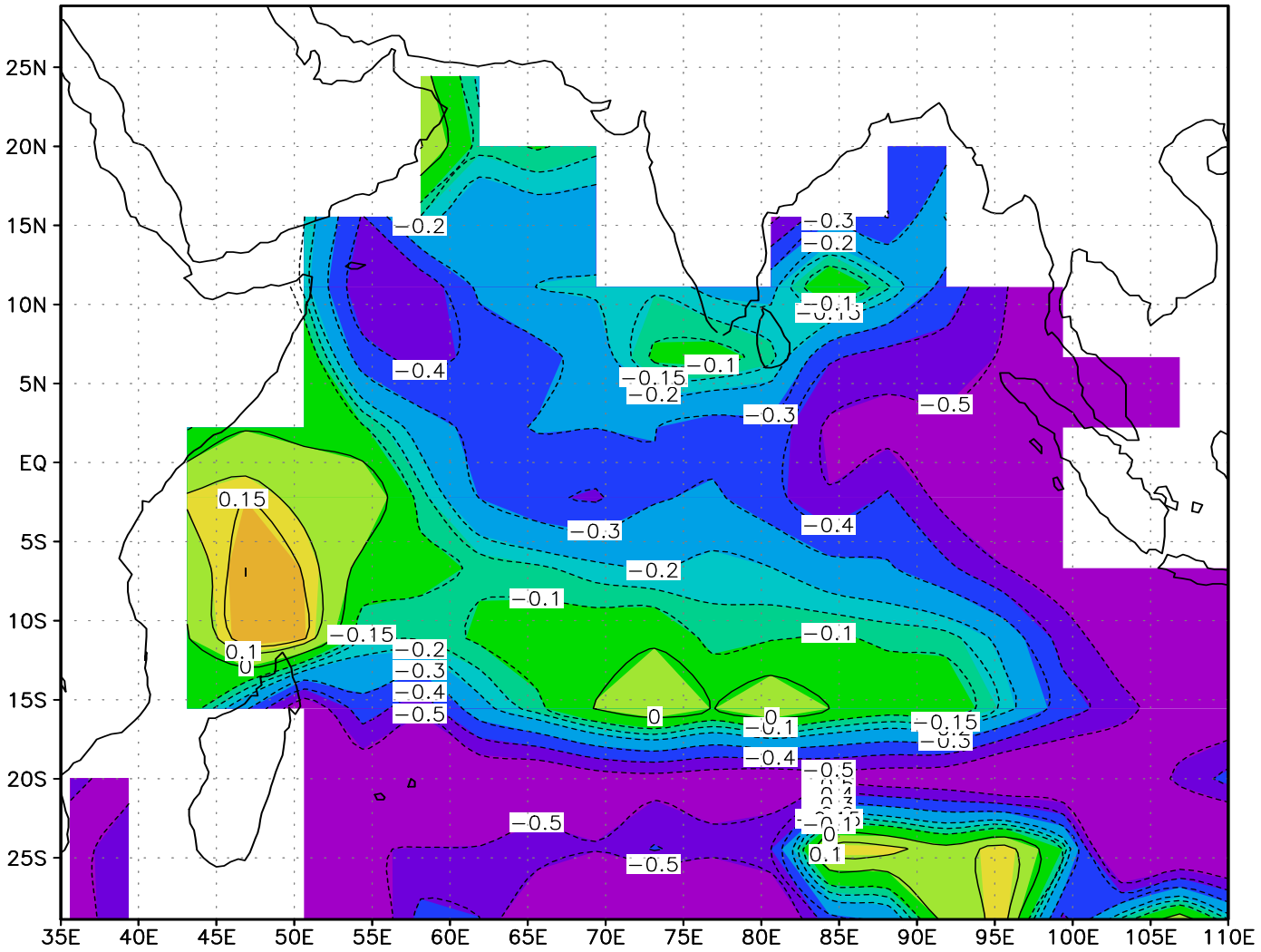

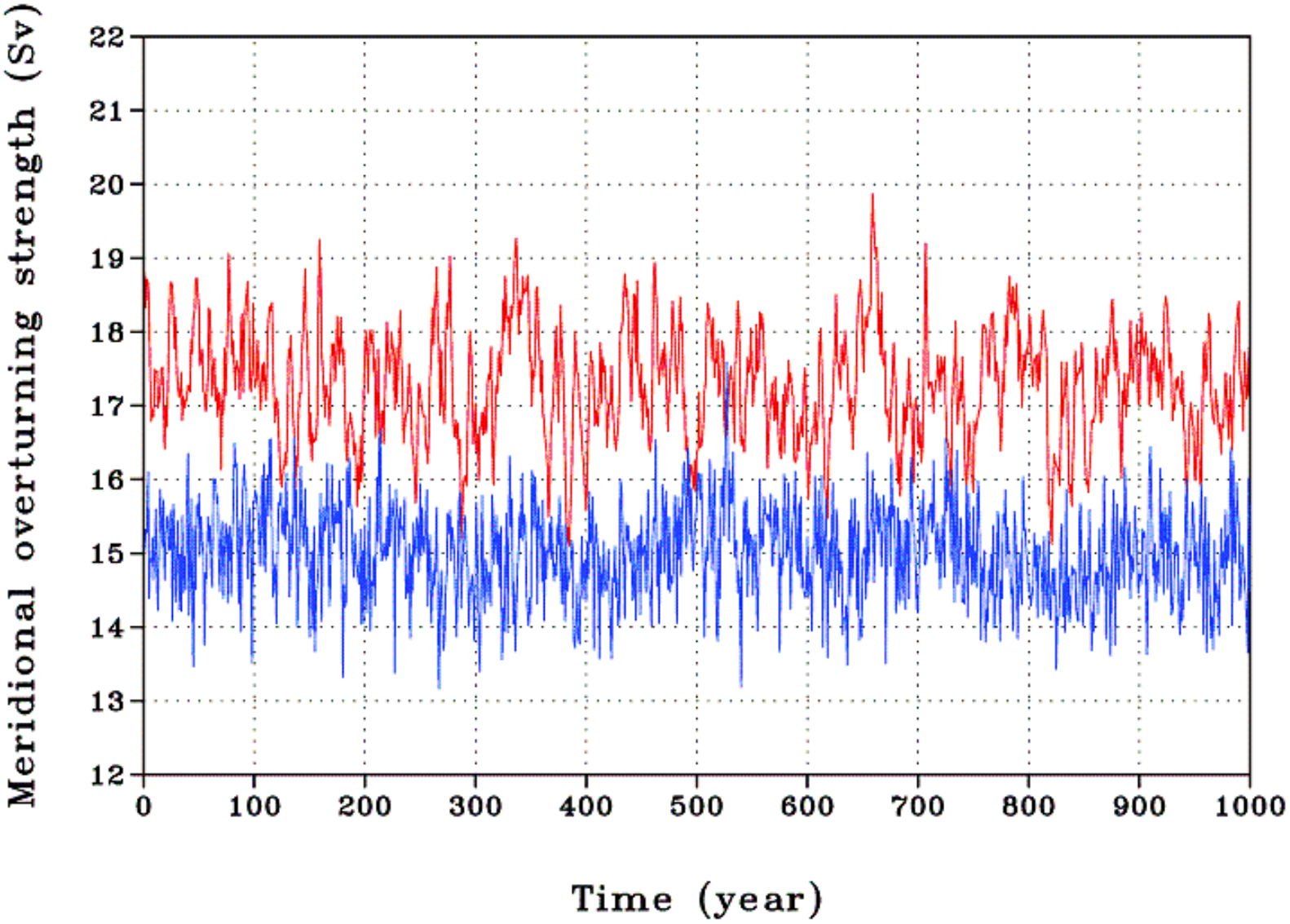
Red: North Atlantic
Blue: Indian Ocean
Meridional overturning strength (Sv)
22
21
20
19
18
17
16
15
14
13
12
0
100
200
300
400
500
600
700
800
900
1000
Time (year)

Summary

- The presence of the decadal IOD.
- The coupled model shows the presence of the ENSO-independent interannual (to multi-centennial) IOD.
- Diagnosis of the physical mechanism of the model decadal event carried out. Similarity with interannual mechanism, with links to the atmospheric circulation on decadal timescales.
- Possible role of Interannual events in decadal IOD.
- The results subject to Data quality problems as well as the coarse resolution of the CGCM.
- Centennial IOD

Proposal to the GLOBAL RESEARCH LAB (GRL) PROGRAM 2007

Interannual Variations of Typhoon/Hurricane Activity in High Resolution Global Climate Models

- A coordinated international project to carry out and analyze high-resolution simulations of tropical storm activity with a number of state-of-the-art global climate models.

- The objectives are (i) to understand the mechanisms that control tropical storm activity on interannual to longer time scales, and (ii) to develop a prediction system capable of foreseeing changes in typhoon activity a season or more in advance.

- Dr. C.-K. Park and Dr. S. Schubert will be the PIs, along with other collaborators.

- Budget Request for seven years: $ 3,500,000 ($500,000 Per year).

Proposal to Global Environment Fund (GEF)

Title: High Resolution Multi-model Forecasts for Adaptation of South Asia to Weather and Climate extremes

Objectives: Two fold: (1) Scientific (2) Capacity Building

(1) Scientific

Utilization of very high resolution MME forecasts, hindcasts, downscaled products and Satellite Data for climate adaptation in developing nations of South Asia by

*(i) **optimizing/improving/building the monitoring network to** predict extreme climate events in advance of 2 weeks and designing the mitigation of the associated losses.*

*(ii) facilitate adaptation to the long term changes in extreme events by **providing river basin-specific dynamic long range seasonal forecasting up to 6 months;** this will aid in water management, mitigate drought and land degradation.*

GEF Proposal (Con'd)

2. Capacity Building

- Capacity building of social, economic and scientific systems to alleviate the impacts of climate change and provide and/or, optimize wherever available, adaptation measures for natural disasters such as typhoons and climate extremes. Capacity building is necessary in each component i.e. (i) Science: improvement of optimal monitoring network /systematic observations, data and modeling techniques to predict weather, climate and other derivatives, such as potential health hazard prediction, at very high resolution. This may involve research and development, and training so as to develop the manpower to manage the developed technology (ii) Dissemination of information: Establishment of efficient network for the dissemination of the information 24/7 and two way communication (from the Scientists and Planners to the end-users, and vice-Versa), and its optimum utilization. This also includes bringing in the existing channels communicate better. (iii) Policy makers: to integrate the high-resolution downscaled MME seasonal forecasts in decision making. (iv) Local users: Agriculture, Forestry, Fisheries, transportation, health, communications etc (v) Human resources development.

GEF proposal (Con'd)

Preliminary Procedure

To apply for the proposal preparation fund.

(i) Identify prospective partners from developing countries in South Asia.

(ii) Organization of a 2-day workshop to identify issues of proposal

(iii) Partial support from other agencies such as ASEAN-ROK would help.

(iv) Interaction with the respective focal points of GEF in Partner countries of South Asia (through partner countries), and procurement of their concurrence that the project suits the national needs. May also be necessary to interact with the focal point of GEF in Korea.

(v) Initiation of the application.

The proposed Role of APCC

APCC will be the *project proponent*, and will submit the initial application for the proposal preparation fund. And help to process/progress the application through the preparing stage. In the execution, APCC will be the technical partner, working closely with the implementation agency (WB, UNDP etc.). We hope to present this proposal under "Multi-focal areas" as a "Full-sized project" i.e. $1,000,000+.